AAPM SCIENTIFIC REPORT

MEDICAL PHYSICS

AAPM Task Group Report 290: Respiratory motion management for particle therapy

Heng Li[1] | Lei Dong[2] | Christoph Bert[3] | Joe Chang[4] | Stella Flampouri[5] | Kyung-Wook Jee[6] | Liyong Lin[7] | Michael Moyers[8] | Shinichiro Mori[9] | Joerg Rottmann[10] | Erik Tryggestad[11] | Sastry Vedam[12]

[1] Department of Radiation Oncology and Molecular Radiation Sciences, Johns Hopkins University, Baltimore, Maryland, USA

[2] Department of Radiation Oncology, University of Pennsylvania, Philadelphia, Pennsylvania, USA

[3] Department of Radiation Oncology, Friedrich-Alexander-Universität Erlangen-Nürnberg, Erlangen, Germany

[4] Department of Radiation Oncology, University of Texas MD Anderson Cancer Center, Houston, Texas, USA

[5] Department of Radiation Oncology, Emory University, Atlanta, Georgia, USA

[6] Department of Radiation Oncology, Massachusetts General Hospital, Boston, Massachusetts, USA

[7] Department of Radiation Oncology, Emory University, Atlanta, Georgia, USA

[8] Department of Radiation Oncology, Shanghai Proton and Heavy Ion Center, Fudan University Cancer Hospital, Shanghai, P. R. China

[9] Research Center for Charged Particle Therapy, National Institute of Radiological Sciences, Chiba, Japan

[10] Center for Proton Therapy, Proton Therapy Singapore, Proton Therapy Pte Ltd., Singapore

[11] Department of Radiation Oncology, Mayo Clinic, Rochester, Minnesota, USA

[12] Department of Radiation Oncology, University of Maryland, Baltimore, Maryland, USA

Correspondence
Heng Li, Department of Radiation Oncology and Molecular Radiation Sciences, Johns Hopkins University, 401 N. Broadway, Baltimore, MD, 21287, USA.
Email: HengLi@JHU.edu

The Chair of the TG290 has reviewed the required Conflict of Interest statement on file for each member of TG290 and determined that disclosure of potential Conflicts of Interest is an adequate management plan. Disclosures of potential Conflicts of Interest for each member of TG290 are found at the close of this document. Reprint permission has been granted for all reprint figures in this task group report.

Abstract
Dose uncertainty induced by respiratory motion remains a major concern for treating thoracic and abdominal lesions using particle beams. This Task Group report reviews the impact of tumor motion and dosimetric considerations in particle radiotherapy, current motion-management techniques, and limitations for different particle-beam delivery modes (i.e., passive scattering, uniform scanning, and pencil-beam scanning). Furthermore, the report provides guidance and risk analysis for quality assurance of the motion-management procedures to ensure consistency and accuracy, and discusses future development and emerging motion-management strategies. This report supplements previously published AAPM report TG76, and considers aspects of motion management that are crucial to the accurate and safe delivery of particle-beam therapy. To that end, this report produces general recommendations for commissioning and facility-specific dosimetric characterization, motion assessment, treatment planning, active and passive motion-management techniques, image guidance and related decision-making, monitoring throughout therapy, and recommendations for vendors. Key among these recommendations are that: (1) facilities should perform thorough planning studies (using retrospective data) and develop standard operating procedures that address all aspects of therapy for any treatment site involving respiratory motion; (2) a risk-based methodology should be adopted for quality management and ongoing process improvement.

1 | INTRODUCTION

1.1 | Purpose and goal

Particle therapy can improve dose distributions over those achieved with photon therapy for patients with malignancies in the thorax and abdomen.[1–4] However, dose uncertainty induced by respiratory motion remains a major concern for treating these patients using particle beams.[5–8] Motion-induced dose uncertainties have been extensively studied in the particle therapy setting,[6,9–14] and strategies such as 4-dimensional (4D) treatment planning,[15–19] rescanning,[6,20–23] breath holding [BH],[24] gating,[25] tumor tracking,[26] and combinations of these techniques[27] have been proposed and implemented at different particle therapy centers. These studies all underlined the importance of implementing proper motion-management techniques to ensure the safety and effectiveness of particle therapy. Additional complexities in particle therapy, such as range-uncertainty considerations, need to be considered in the overall motion-management strategy compared to photon beam treatment.[28] Therefore, guidance is required on choosing the proper motion-management techniques and how to implement a motion-management program in the context of particle-beam delivery. The purpose of this Task Group, TG-290, was to review existing and emerging motion-management techniques in particle therapy, emphasizing implementation and quality assurance (QA). To this end, the AAPM Therapy Physics Committee formed TG-290 with the following charges:

1. To review the impact of tumor motion and dosimetric considerations in particle radiotherapy.
2. To review current motion-management techniques and their limitations for different particle-beam delivery modes (i.e., passive scattering [PS], uniform scanning [US], and pencil-beam scanning [PBS] delivery modes).
3. To provide guidance and risk analysis for QA of the motion-management procedures to ensure their consistency and accuracy.
4. To discuss the future development of emerging motion-management strategies.

This report will describe the effect of respiratory motion on particle therapy delivery, review current motion-management techniques, and provide recommendations for their implementation.

1.2 | Scope

This report discusses respiratory motion-management related topics that are considered crucial to the accurate and safe delivery of particle therapy. In general, it does not discuss problems common to both photon and particle therapy such as target delineation. A brief review of cardiac motion and its impact on radiation therapy, particularly particle therapy, is included as an Appendix 1, but not discussed otherwise in this report.

2 | NOMENCLATURE AND DEFINITIONS

The nomenclature and definitions used in this report follow those used in ICRU Report #78, "Prescribing, Recording, and Reporting Proton-Beam Therapy,"[28] AAPM Monograph #37, "Principles and Practice of Proton-Beam Therapy,"[29] and recommendations made by NRG Oncology[30] and AAPM.[31] Additional terms relevant to motion management, in particular for particle therapy, are defined as follows:

For the purpose of this report, breathing and respiration are used interchangeably.

In general, motion-management techniques can be categorized as either passive or active. *Passive motion-management techniques* (e.g., additional target margins, 4D treatment planning, or rescanning during treatment delivery for PBS) generally involve freely breathing patients. They do not regulate the beam delivery according to the patient's respiratory state. In contrast, *active motion-management techniques* (e.g., BH, gated treatment, or tumor tracking) regulate patient breathing and/or treatment delivery according to the patient's respiratory state.

BH treatment describes approaches to manage respiratory motion during particle-beam delivery by "inhibiting" such motion, with (*voluntary BH*) or without (*involuntary BH*) active cooperation from the patient.

Gated treatment describes techniques that limit particle-beam activation to the *gating window*, a predetermined portion of the respiratory cycle. Patients are usually treated under free-breathing gating (FB-gating) using this technique.

The interplay effect describes the dosimetric impact that stems from the interaction of the dynamic particle-beam delivery with the patient's internal motion. The interplay effect is of particular concern for PBS delivery due to the potential severity of the impact and the difficulty in predicting its magnitude. The difficulty is primarily due to the random components of routine procedures such as variation in the starting phase of the breathing cycle, variation in the breathing cycle itself, and delivery system variations in switching time and dose rate. As a result of the interplay effect, the actual delivered dose of each fraction in the treatment course could be different from the plan and each other.

The robustness of a treatment plan describes the degree to which the desired dose distribution is resilient to various uncertainties.[32] The uncertainties to be

considered include information within planning images and models, limited machine precision, geometrical errors from patient setup, range uncertainties in particle therapy, anatomy changes throughout treatment, and specifically, motion robustness.

The *static dose* is the dose calculated from a single computed tomography (CT) data set, be it the average CT, midventilation CT, or FB CT.[33]

4D accumulated dose or *4D dose* (4DD) is the weighted average of the doses calculated on either selected or all (typically 10) individual phases of a 4D CT simulation scan using the planned delivery sequence. 4DD is calculated using only the treatment plan and 4DCT image set without considering the time dependence of the delivery fluence.[34]

Dynamically accumulated 4D dose (D4DD) or *dynamic 4D dose* (dynamic 4DD) considers the time-dependent delivery sequence or radiation fluence together with representative anatomic motion (determined using tools such as 4DCT or 4DMRI [4D-magnetic resonance imaging]). The summed or fraction-averaged D4DD tends to converge to the 4DD when multiple deliveries or fractionations are considered.[35]

4DD and D4DD could be calculated using selected phases; examples include phase-based gated treatment using a predefined gating window.[36,37] In such cases, the phases used for dose calculation should be clearly defined.

4D treatment planning is an extension of the conventional 3D treatment planning, where the 4D image dataset, sometimes along with the timing of the treatment delivery, is used to calculate or evaluate the dose to moving targets and organs at risk (OARs).[38]

> 4DD and D4DD are typically used in 4D treatment planning and motion robustness evaluation.

Rescanning or *repainting* is a simple PBS delivery-based technique used to minimize the dose uncertainty caused by the interplay effect: the same spot pattern is delivered multiple times. Rescanning techniques can be based on 2-dimensional (2D)(layered) or 3D (volumetric) rescanning.

(Discrete) spot scanning is a PBS delivery mode in which the dose is shaped by changing the number of particles at a specific location defined by the scanning magnets and energy of the beam. The beam is off between different beam locations (spots) in spot scanning mode, whereas the beam remains on between spots in the raster scanning delivery mode.[39]

Continuous scanning (line scanning), on the other hand, is a scanning delivery mode in which the beam remains on during scanning with variable beam intensities and speeds.[40] In continuous line scanning mode, the spot concept is usually no longer valid. However, one could still use control points or control spots to describe the beam parameters such as beam off during scanning as needed. These scanning delivery techniques can deliver intensity-modulated particle therapy (IMPT) with a highly conformal dose. However, different scanning methods require additional considerations when implementing motion-management procedures due to the time-structure difference in the delivery.

Water-equivalent thickness (*WET*)*, water equivalent depth* (*WED*), or *water-equivalent-path-length* (*WEPL*) are terms used to describe the energy loss of the particle beam as it penetrates specific material and is scaled to water. WEPL can be calculated by integrating the relative stopping power (RSP) to water over the particle beam. The change in WEPL (ΔWEPL) between different CTs (e.g., different phases of 4DCT) can be used to quantify the possible dosimetric impact of inter- and intrafractional change between the CTs to an incoming particle beam.

3 | BACKGROUND

3.1 | Respiratory motion

Breathing, a complex physiological process, causes tissue motion, transient deformation, and density variation in the thorax and abdomen. The tumor motion range associated with respiration is specific to each patient but generally depends on the tumor location and disease stage. A review of the respiratory motion literature concluded that no general pattern of respiratory behavior could be assumed for a patient before observation and treatment.[41] Thus, individualized imaging of tumor motion is highly desirable in both simulation and treatment.

Representations of respiratory motion can be captured with 4DCT by sampling the patient volume over time, thus, creating a dynamic volume data set.[42] Analysis of 4DCT images of non-small cell lung cancer (NSCLC) tumors correlated tumor motion characteristics with tumor location, volume, and clinical staging.[43] The largest tumor movements occurred in the lower lobes of the lung, in the superior-inferior direction, and were associated with diaphragm motion. Early-stage NSCLC tumors had a range of motion of up to 30 mm, whereas the range of motion of locally advanced tumors seldom exceeded 10 mm.

Tumor and organ motion in the abdomen has also been measured using MRI,[44–47] 4DCT,[48–50] and real-time tracking of fiducials implanted near the tumor.[51,52] These methods determined that tumor motion occurs in all three spatial directions, generally showing greater magnitude in the superior-inferior direction.[53]

For particle therapy, in addition to tumor motion, variations in tissue thickness or density along the beam path can affect the dose distribution in the patient. For example, the combination of chest wall thickness variation and target position variation in lung treatments could lead to dose distribution deviations from the initial plan.[54]

3.2 | Dosimetric impact of respiratory motion in particle therapy

The finite range of a particle and its dependence on the density and composition of the tissues that it traverses, in combination with patient breathing, results in unavoidable effects on particle therapy dose distributions. This section briefly describes dose perturbations caused by respiratory motion and tissue-density changes under the assumption that neither the dose delivery nor patient respiration is regulated. Statistical analysis of the dose delivery process and respiratory motion can categorize the dosimetric impact of respiratory motion—or the dose uncertainty induced by motion—into systematic and random components.[55]

The systematic component of the dosimetric impact from respiratory motion stems from the difference between the static CT dataset used for treatment planning and the dynamic nature of the actual patient geometry during treatment delivery. Ideally, the dynamic patient geometry could be described by the 4DCT; thus, the systematic difference could be quantified by the difference between the static and 4D doses. The severity of the systematic difference depends on (1) the magnitude of the variations between the 4DCT and the conventional (or 3D) CT on which the static dose was calculated and (2) the ability to account for these variations during treatment planning and delivery processes.

The random component of motion-induced dose uncertainty, which is often referred to as the interplay effect, is caused by the interaction of the dynamic particle-beam delivery with the target's motion, resulting in local dose heterogeneities within the target.[6,10,12,56] For beam delivery during FB, beam delivery, and patient breathing can generally be viewed as independent processes; thus, the complex effect can be described as a spatial and temporal combination of beam delivery and patient breathing for individual pencil beams. Timings of both beam delivery and breathing are additionally required to predict and evaluate the interplay, which may encompass on- and off-target effects due to the motion of the CTV. Interplay may have more severe consequences for PBS with organ motion than intensity-modulated (photon) radiotherapy (IMRT), because the static dose cloud approximation[41,57] that applies to IMRT is not valid for particle therapy. Instead, the dose gradients for PBS are sharp in all three dimensions, and the interplay effect can be amplified by scanning of spots. Dynamic 4D dose considers beam delivery and breathing timing and is often used to quantify the interplay effect.[11,12,21,34,58] For more accurate estimation of interplay effects along heterogeneous beam paths, Monte Carlo (MC)-based dose calculation is preferred over analytical-based techniques.[59–61]

Both the 4DD and the D4DD incorporate respiratory motion, but they do so differently and require distinct or overlapping considerations. The 4DD is a more straightforward calculation because it assumes that the dose is evenly distributed in the selected motion phases of the 4DCT underlying the calculation. On the other hand, D4DD considers both the patient's respiratory and the delivery timing information. As a result, 4DD is the same for all fractions, and D4DD could be different among fractions. It is also noted that both 4DD and D4DD were calculated on the simulation 4DCT, which captures patient breathing motion at the time of acquisition. The implicit assumption that a patient breathes the same way throughout treatment may or may not be a valid one.[62,63] It is, however, currently challenging to test the hypothesis with real-time patient breathing data.

Using a simplified model, Figure 1 summarizes three scenarios where respiratory motion impacts dosimetry and highlights the unique challenges for particle therapy. Figure 1a shows a simple motion model with two phases (T0 and T1), where the target (red circle) did not move, but the high-Z (e.g., bone) structure that was anterior to the target moved laterally. The average CT (AVG) was generated by taking the average of the two phases. The figure shows that a single anterior-posterior particle beam must pass through the moving structure to cover the target.

A 3D treatment plan was created on the AVG image, as shown in Figure 1b, using a single spot (yellow spot). The dose from the spot was calculated on AVG, and the target received the full dose. However, when the dose was recalculated on T0 and T1, the target coverage deteriorated because of the WEPL change of the particle beam between AVG and T0/T1. Note that doses for this particle beam were shifted along the beam direction (or depth direction) only for AVG, T0, and T1 dose, and the shift was determined by WEPL change. 4DD on T1 was calculated by deforming the T0 dose to T1 and taking the average of the two dose distributions on T1. The two yellow spots, each with half of the area of the original spot, denote the contribution to the 4DD from individual phases (T0/T1) of the same spot, and their Bragg peak range location relative to the target (that was deformed to T1) on individual phases. The target coverage on 4DD also deteriorated.

In comparison, a 4D treatment plan was created on both T0 and T1, as shown in Figure 1c, using two spots (purple and green). The target was sufficiently covered in the calculated dose distribution on both T0 and T1, but the dose on AVG was suboptimal. The target also received full coverage on the 4DD of the 4D plan, where the two spots were shifted along the beam direction, and the amount of shift was again determined by WEPL change.

D4DD of the 4D plan, as shown in Figure 1c, was calculated in Figure 1d. Assuming the delivery to the two spots were independent of each other, there were a total of four scenarios of possible outcomes for the dynamic dose calculation of the two spots: (1) spot 1 (purple) was delivered to T1 and spot 2 (green) to T0, (2) spot 1 to T1
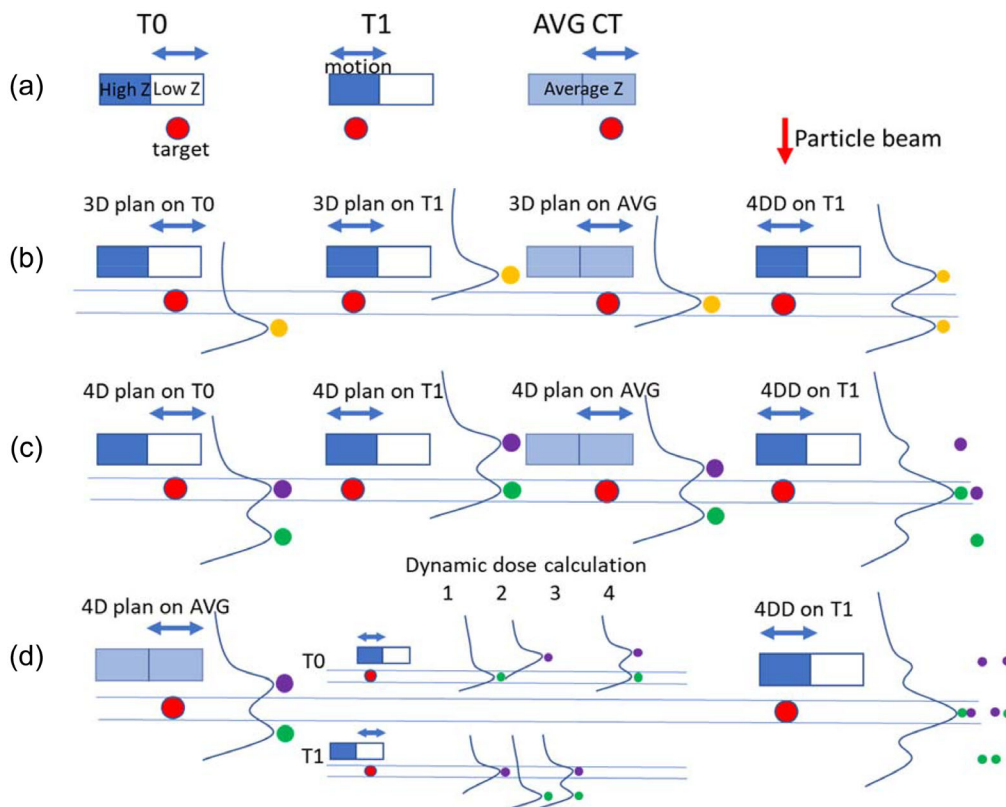
FIGURE 1 Dosimetric impact of motion on particle beam. (a) A two-phase respiratory motion model, where the target did not move, but the high-Z (bone) structure moved in and out of a single particle beam. The average image (AVG) was generated by taking the pixel-by-pixel average of the two phases (T0 and T1). (b) 3D plan that was created using AVG, where a single spot (yellow) was used. The dose distribution for the same plan was then recalculated on both T0 and T1. The 4DD was then calculated by deforming dose distributions onto T1, and taking the average of all deformed doses. (c) 4D plan was created using both T0 and T1, where two spots (purple and green) with different energies were used to ensure coverage on both phases. The dose was then recalculated on AVG, and 4DD was also calculated. (d) Dynamic dose calculation for the 4D plan was simulated. For two spots and two phases, there were four possible dynamic delivery scenarios. Assuming the two spots were delivered independently and to each phase with equal chance, the weighted average of the four possible scenarios yielded the same result as 4DD

and spot 2 to T0, (3) both spots to T1 and (4) both spots to T0. Assuming the patient spent equal time in T0 and T1, each of the four scenarios had an equal chance to occur. Note that due to the interplay effect, in scenario 2 of the dynamic delivery, the target coverage deteriorated, and in scenario 1, the target overdosed. With treatment with single delivery (fraction), there was a 25% chance of underdosing the target and a 25% chance of overdose. With multiple deliveries (fractionation), the dose for each delivery would be one of the four scenarios, and the accumulated dose would be the sum of these deliveries. This simple case showed that more fractionation decreased the chances of an extreme scenario, where the target was underdosed or overdosed in the accumulated dose, with multiple fractions. Furthermore, the expectation of the dynamic deliveries became the weighted average of the four scenarios and was identical to the 4DD.

While heavily simplified, Figure 1 highlights the challenges of motion management for particle therapy. In this 2D example, the target was stationary, there were only two phases, two spots, and the delivery timing of the spots was not considered. Actual patients are much more complicated, with the need to consider tumor motion, a 4DCT with multiple phases, and a plan consisting of multiple beam angles, tens of energies, and tens of thousands of spots with a delivery time of minutes. It is, therefore, essential to fully understand the basic concepts that are illustrated with this simple example before tackling real-life challenges:

1. WEPL variations, along with tumor motion, are essential for motion evaluation in particle therapy.
2. The systematic difference between 3D and 4D doses cannot be resolved by fractionation or rescanning. 4D planning may mitigate the problem of 4D dose deterioration.
3. The interplay effect, due to its random nature, can be mitigated by fractionation or rescanning.

It is also worth noting that the interplay effect can be evaluated by using dynamic 4D dose but not 4D dose,

which does not consider the delivery process of the treatment plan.

4 | REVIEW OF CURRENT MOTION ASSESSMENT AND MOTION-MANAGEMENT TECHNIQUES FOR PARTICLE THERAPY

4.1 | Overview

Current motion-management techniques can be categorized into passive and active techniques. Three surveys on motion management for particle therapy were conducted via private communication in 2014, 2016, and 2018, with results summarized in Appendix 2. The surveys showed the evolution of motion management over the past decade and some current trends. Some commonly used passive motion-management techniques for PS and US include target CT number overrides for range compensator design and smearing (thinning of the compensator). These techniques usually reduce the conformity of the beam to the distal edge of the target but ensure target coverage under motion and setup errors. For PBS, adding margin along the beam, increasing the beam spot size, altering the scanning and delivery pattern or mode, and decreasing spot spacing can diminish the deleterious effects of motion. Active motion-management techniques are used to reduce the effective range of motion and can be used with passive motion-management techniques. As described in Section 4.7, robust optimization is a treatment planning strategy that allows the user to explicitly include anticipated uncertainties such as geometric targeting errors, range uncertainties, and incorporation of multiple planning CT scans. The adequacy of any remedy for motion-induced error is usually evaluated by motion robustness analysis.

4.2 | Tumor motion and beam angle-specific WEPL evaluation

4DCT, or respiration-correlated CT,[42] has become the de facto standard for tumor motion visualization and is widely used for treatment simulation and planning for thoracic and abdominal malignancies.[64,65] 4DCT could be used to better determine the extent of anatomic motion in an individual patient compared to a FB CT, and is routinely used for target and critical structure delineation in radiotherapy planning. It is often supplemented with other imaging techniques, such as FB/BH CT, positron emission tomography/CT, MRI, and fluoroscopy. Deformable image registration (DIR) could be used for quantitative motion evaluation with 4DCT. For example, the deformable vector fields generated by deformable registration of the inhale (T_0) and exhale

(T_{50}) phases of the simulation 4DCT could quantify patient motion on a voxel-by-voxel basis.

4DCT or multiple CT datasets have been used to calculate the difference between the WEPLs (ΔWEPL) needed to ensure target coverage. It was demonstrated in several studies that[54,66] ΔWEPL was highly patient-specific, depending on the beam angle, and was positively correlated with dose variation from the plan. Therefore, patient-specific ΔWEPL analysis could be used for beam angle selection—for example, as shown in Figure 2, beam angles with the smallest ΔWEPL between 4DCT phases are considered the most robust toward motion-induced dose uncertainties.[1,34,67,68]

ΔWEPL can be calculated as follows[1,69]:

1. For each beam angle, identify the distal surface of the target volume.
2. In the beam's eye view, for each beam angle, calculate the WEPL by using an equation such as equation (1) (adapted from Siddon et al.[70]). In the equation, $d(x,y,z)$ is the distance in the voxel that is traversed by the particle pencil beam, and $RSP(x,y,z)_{material}$ the RSP of the material in the same voxel.

$$WEPL = \sum_x \sum_y \sum_z d(x,y,z) \cdot RSP(x,y,z)_{material}.$$

(1)

3. Calculate the ΔWEPL as the difference between the WEPLs required to cover the distal surface of the same target volume on different CTs, for example, the ΔWEPL between the inhale and exhale phases on 4DCT simulation.
4. Perform the above calculations for all relevant beam angles (e.g., full gantry rotation of 360°).

4.3 | Particle therapy delivery modes

Currently, accelerators for particle therapy are either a synchrotron, which extracts spill-structured beams, or a cyclotron (or synchrocyclotron), which extracts quasi-continuous beams.[71,72] The beam extracted from the accelerator usually is a quasi-monoenergetic beamlet with narrow energy and spatial distributions. Therapeutic cyclotrons extract fixed-energy particle beams, whereas therapeutic synchrotrons extract a predefined set of discrete energies within a range. Beam energies in both systems can be adjusted using range shifters. Several delivery techniques have been developed to generate desired dose distributions and ensure coverage of the entire tumor volume by the extracted beam. However, different types of accelerators and delivery modes interact differently with patient respiratory motion; therefore, these factors need to be considered when developing a motion-management program.

Currently, three commercial delivery modes are available: PS systems, including single-scattering and
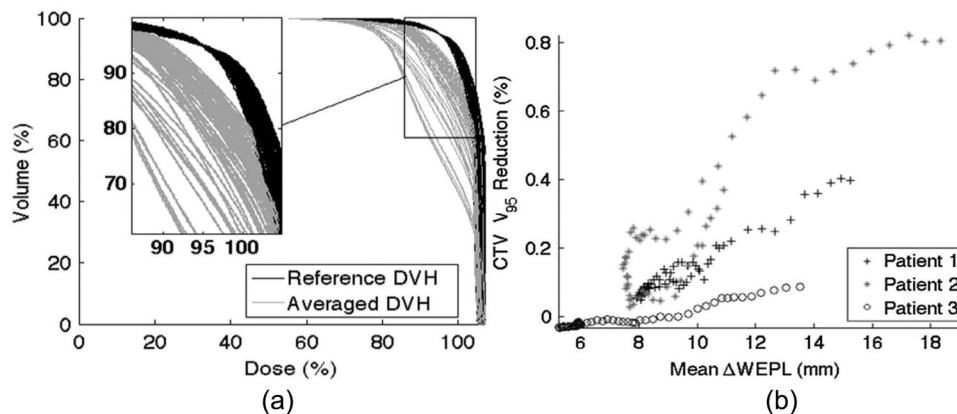
FIGURE 2 (a) Reference MIP DVH (black) and phase averaged 4DCT DVH (grey) for the ITV for 61 single-beam plans for patient 1. The plans were normalized to obtain V95 = 95%, as can be seen in the zoom region, where all reference DVH cross this point. Doses and volumes are given as a percentage of the total. (b) Scatter plot for patients 1 to 3 showing the strong association for each patient between the V95 reduction with the mean ΔWEPL. The values for the linear correlation coefficients are 0.98, 0.92, and 0.96 for patients 1, 2 and 3, respectively ($p < 0.01$). ([a] Figure 1 and [b] Figure 5 from Oscar Casares-Magaz et al., A method for selection of beam angles robust to intrafractional motion in proton therapy of lung cancer. Acta. Oncol. 2014;53(8):1058–1063. Note that the (%) reduction in (b) appears to be decimal)

double-scattering systems; US systems; and PBS systems. PS and US delivery systems generate 3D homogeneous dose distributions in clinically acceptable sizes by modulating the particle beamlet in lateral and depth directions. The broadened beam is then conformed laterally to the beam's eye-view shape of the tumor using physical apertures and conformed distally using range compensators. In contrast, PBS uses individual beamlets deflected by scanning magnets in two orthogonal planes perpendicular to the beam axis. The final dose distribution is formed by adjusting both the integrated flux and the location of beamlets of different energies to cover the depth direction of the target volume. For stationary targets, PS and US deliver effectively the same dose distribution, whereas PBS could have dosimetric benefits, as the dose from PBS can be more conformal in the proximal aspect of the target volume and, thus, reduce the dose to OARs.

However, because of their different methods for spreading the beam over the target volume, PS, US, and PBS have different delivery time structures that interplay with respiratory motion differently. As shown in Figure 3, a DS delivery system spreads the beamlet laterally via scatterers and can spread proximally and distally (energy/range) via rotational modulation wheels; therefore, the volumetric dose is delivered with the rotation of the wheel (25–100 ms per delivery of volumetric dose). Alternative options for spreading proximally and distally in scattering beams include variable range shifters and ridge filters (not shown in Figure 3), leading to the same delivered dose in a stationary target but having different delivery time structures. For a US delivery (Figure 3 middle panel), the beam is spread laterally through fast continuous scanning of the spot at each energy. Still, after each energy is delivered, a short time is required for energy switching (scanning on the proximal-distal direc-

tion), from tens of milliseconds to a couple of seconds. Again, different implementations of the US can lead to the same dose distribution with different delivery time structures. For PBS, especially discrete spot scanning in which the beam is paused at each spot location, the delivery time depends on the number of spots for each layer, the number of layers, and the energy-switching time. Therefore, PS is usually considered the least sensitive to motion, PBS the most sensitive, and the US in between.[73] More details about each delivery technique are discussed in Section 4.4.

4.4 | Passive motion-management techniques

4.4.1 | General techniques

Motion-management techniques incorporated at the treatment planning level may be applied regardless of the delivery mode (DS, US, PBS). These techniques include adequate beam angle selection as discussed in Section 4.2 and motion encompassing techniques that expanded the treatment volume to ensure sufficient target coverage throughout the observed breathing phases (e.g., via 4DCT). This approach assumes that the 4D planning CT represents the patient's respiratory organ motion and anatomy throughout the treatment delivery. However, this assumption may not always remain valid due to variations in breathing patterns and anatomical changes such as tumor shrinkage or weight loss over time. As discussed in Section 3.3 for particle therapy, dose distributions are particularly sensitive to density changes in the beam path, for example, caused by respiration, which can influence the beam range. Treatment planning on the average CT can mitigate some of these
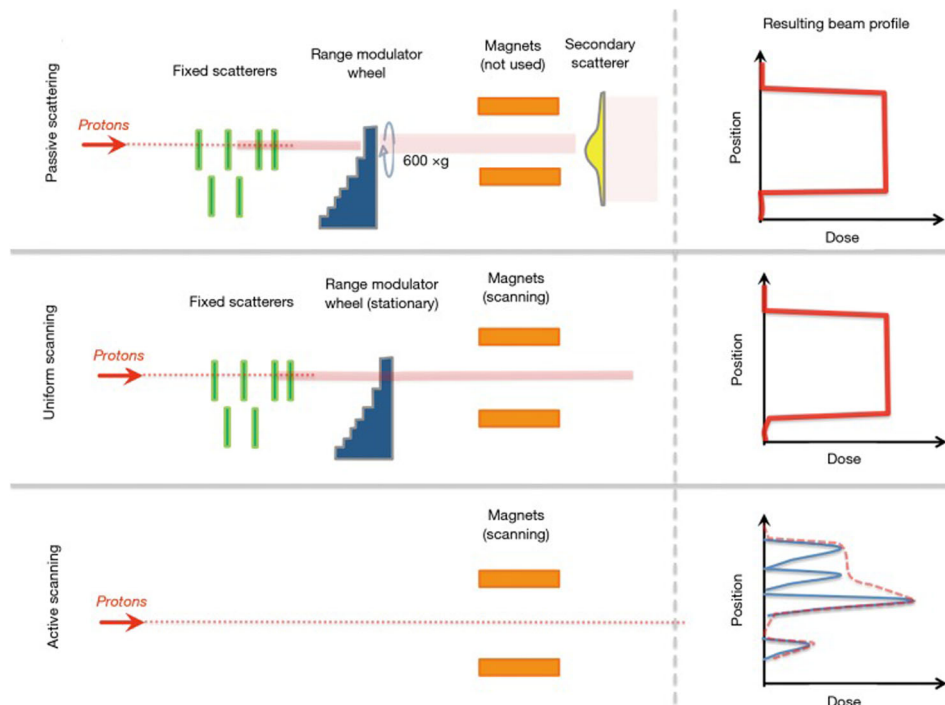
FIGURE 3 An illustration of the hardware differences between passive scattering (top), uniform scanning (middle panel), and active scanning (a synonym for PBS) modalities. For active scanning (bottom row), the resulting radiation field is the sum of all of the individual spots, which may have different intensities. In the illustration, each spot contributes to the total dose indicated by the red dashed line. (Figure 2 from James SS, Grassberger C, Lu HM. Considerations when treating lung cancer with passive scattered or active scanning proton therapy. Transl. Lung Cancer Res. 2018;7(2):210–215)

effects. Additionally, a Hounsfield unit (HU) override of the target volume with a HU number representing the average HU of the volume can provide increased distal coverage, yet may also increase the dose to tissues adjacent to the distal edge including OARs.[34,74]

4.4.2 | Techniques applicable to PS

Compensators are used in both PS and US to conform the distal end of the beam to the target. Margins can be used to account for range and motion uncertainties by changing the thickness distribution of compensators. In particular, a technique to account for lateral positional or motion uncertainties called "expansion" or "smearing" is used in compensator design. The compensator smearing approach applies the thinnest compensator thickness to all neighboring compensator positions within a search radius,[75] so that in the case of lateral positional change or motion, the distal end of the target still receives full coverage.[76]

One specific consideration for treatment planning with PS delivery is that this technique typically entails a negligible interplay effect. Therefore, PS delivery can be considered for treating patients with relatively large motion (i.e., greater than 10 mm) who require fewer fractions (i.e., fewer than 5). However, the inability to control the

relatively larger proximal treatment margin might limit the application of PS delivery due to the risk of excessive toxicity in OARs proximal to the target.

4.4.3 | Techniques applicable to the US

The US is a beam delivery technique that spreads the beam laterally across the target, and it provides a lateral dose profile similar to that achieved by the DS technique.[77,78] US was first used with proton beams in 1958[79] and was extensively used with electron beams during the 1970s and 1980s.[80] A description of various scan patterns that have been used for particle beam therapy is provided in Moyers and Vatnitsky.[81]

When the US is used with particle beams, it is usually performed with a static range modulator (such as a ridge filter), or in concert with the energy stacking technique. When a ridge filter is used for range modulation, the entire target volume is covered within a fraction of a second. Dose blurring becomes the dominating phenomenon resulting from respiratory motion, similar to PS delivery. On the other hand, the energy stacking technique sequentially delivers each of the multiple energies required to cover a target uniformly. With this technique, each energy step may take from one to several seconds to deliver, and thus, interplay effect is of concern, similar
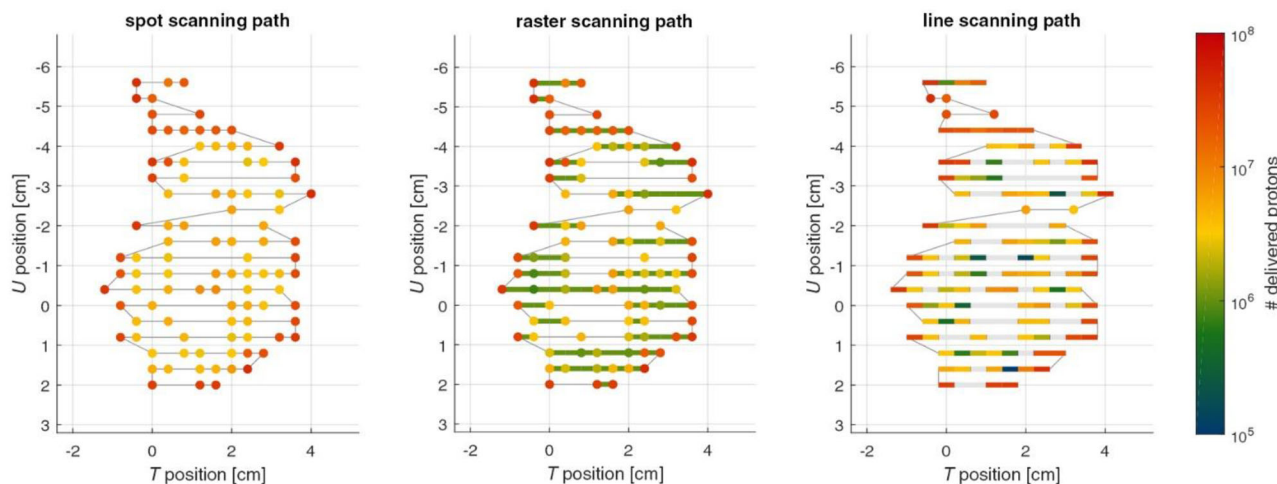
FIGURE 4 Illustration of the scan path within an energy layer for the three scanned particle delivery techniques: spot scanning, raster scanning, and line scanning (from left to right). Axes T and U span the energy iso-layer plane. Klimpki et al. Phys. Med. Biol. 2018;63:145006. https://doi.org/10.1088/1361-6560/aacd27

to PBS delivery. To partly mitigate the problem, miniridge filters can be placed in the beam path to effectively deliver several energies at one time through the process of range shifting. This technique reduces the number of energy levels delivered by the accelerator (and thus the energy selection system). It keeps spots tightly packed in the depth direction, minimizing local over- and under-doses, even under the influence of tissue motion.

4.4.4 | Techniques applicable to PBS

As described in Section 2, scanning beam delivery can be implemented using three different techniques: discrete spot scanning,[82,83] raster scanning,[84] and continuous (line) scanning.[85,86] These techniques are illustrated in Figure 4. Compared to spot scanning, both raster and continuous scanning can reduce the scan time per isoenergy layer (and consequently also the volume scan time) by eliminating dead (beam-off) time between discrete spots.[12,87–89] Speeding up the delivery could enable more rescanning within the same treatment time.[90] Furthermore, the variation of scan speeds can make the gating period match the beam-on period achieved by modulation of the raster scanning speed and beam intensity. Variable scan speeds can allow for time synchronization between delivery and breathing (BH or gating) in real time.

Beam-specific planning target volume (BSPTV)
Beam-specific planning target volume (BSPTV) method developed by Park et al.[91] explicitly includes the variation of WEPL along each beam direction. While the results for BSPTV and smearing are similar for PS, the BSPTV can be used in single-field optimization for PBS planning. In the BSPTV method, distal and proximal water-equivalent treatment margins are con-

verted to geometric treatment margins (GETM) that are calculated according to local tissue heterogeneity. The GETMs are then added beyond the target to approximate a smearing effect in PBS. The GETMs help account for WEPL variations related to the fixed value of tissue misalignment caused by motion and setup.

Rescanning
The interplay effect between pencil-beam motion and organ motion in PBS treatment deliveries may be partially mitigated by rescanning. This strategy will wash out interplay-induced hot and cold spots and approximate the 4D (accumulated) dose distribution defined in Section 2.[6] Figure 5 illustrates various rescanning techniques. Rescanning strategies may be grouped into either 3D volumetric rescanning (VS) or 2D layered rescanning (LS). During VS, the entire volume is scanned in each rescan, while during LS, a single energy layer is scanned multiple times before the next energy layer is applied.[92] Breath sampled LS techniques spread the layer rescans out over the entire breathing cycle. The technique has been shown to yield similar or superior results compared to VS and simple LS, even with typical breathing pattern variations of up to 20%.[11,93] While only breath sampled LS is shown in the figure, the principle of correlating beam scanning with patient breathing could indeed be generalized and applied to VS.[11] Specifically, first proposed by Furukawa et al., phase-controlled rescanning (PCR), where the particle beam finishes one pass of scanning in each of the phases, was implemented at National Institute of Radiological Science (NIRS) of Japan. PCR was studied in both gating and nongating settings,[88,94,95] and it demonstrated the capability to mitigate interplay effects efficiently.

It should be noted that the efficacy of the rescanning techniques is sensitive to the timing of the rescans with respect to the patient's breathing motion.
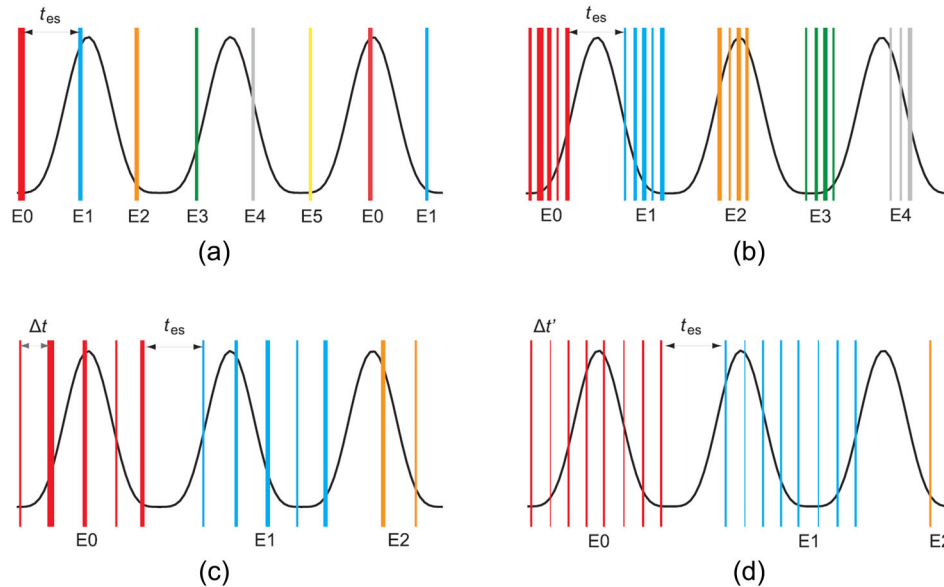
FIGURE 5 Rescanning strategies: (a) volumetric rescanning, (b) layered rescanning, (c) breath sampled layered rescanning, and (d) continuous breath-sampled layered rescanning. The energy switching time, t_{es}, is dictated by the machine, while the time delay between the layers, Δt, is introduced in the breath-sampled techniques to spread the layer rescans of an energy level over the full breathing cycle (line thicknesses illustrate the relative weight of each layer). Engwall et al. Phys. Med. Biol. 2018;63: 095006. https://doi.org/10.1088/1361-6560

To achieve the 4D dose in a single fraction, the dose of each layer needs to be spread out evenly over all breathing phases (Figure 5). Therefore, breathing pattern regularity, tumor volume, and motion range need to be considered. Adjustments also should be considered for the PBS delivery system characteristics, such as energy layer- switching time t_{es} and in-layer scanning speed, which in turn is limited by parameters such as beam current and dose rate.[12,58,96,97] The scan time for the full target volume is approximately proportional to $\propto N_{rs} \cdot t_{es} \cdot \sum_{layers} t_{layer}$, where N_{rs} is the number of rescans and t_{layer} is the approximate time to deliver a layer during each rescan (neglecting per-layer delivery time variations). The energy-switching time is, therefore, highly relevant in determining the efficiency of VS.

The minimal deliverable number of monitor units (MUs) per spot imposes a machine-specific limit on the number of rescans for a spot—independent of the employed rescanning technique. However, particular IMPT plans may feature large spot weight variation on the order of 30:1, which exacerbates this issue.[40] Splitting each spot into a fixed number of rescans is commonly referred to as scaled rescanning.[6] When utilizing this technique, the number of rescans is limited by the smallest spot weight in each energy layer and the minimal deliverable spot weight of the PBS systems. Alternatively, an iso-LS scheme may be employed, which indicates that a fixed number of MUs is applied to each spot during each rescan.[20] This rescanning scheme results in more rescans for higher weighted spots than for lower weighted spots and has proven clinically viable on current hardware.[17,20] Breath sampled LS

can decrease layer doses over the breathing cycle as the final rescans contain fewer spots. This discrepancy can be mitigated by randomizing the rescan delivery order. More extensive target motion ranges required more rescans to approximate the 4D dose with a single fraction delivery.[23] While the effectiveness of rescanning was often evaluated using repeated D4DD calculations,[98] Li et al. recently proposed to use an analytical model to avoid the repeated calculation.[99]

Spot spacing and spot size modification
Sensitivity to interplay increases with increasing spot spacing as well as decreasing spot size.[9,23,100] This effect can be intuitively understood by the decrease in spot overlap when reducing spot size and/or increasing spot spacing. A tradeoff exists in that smaller spot sizes result in a relative sharpening of the lateral penumbra and, hence, provides a better normal tissue sparing,[1,101] at least for more superficial target or plan geometries. Therefore, there is a trend among newly commissioned proton therapy facilities toward smaller spot sizes.

Optimization techniques
Compared to PS and US, one advantage of the PBS technique is shaping the dose distribution with inverse planning or optimization techniques.[102] Robust optimization takes setup and range uncertainties into account to provide treatment plans with better target coverage.[103,104] 4D optimization aims at incorporating respiratory motion into the treatment-plan calculation.[18] The combined 4D robust optimization may additionally take the spot delivery timing into account to

simultaneously also mitigate interplay effects. However, the efficacy of 4D robust optimization depends on the stability of the delivery time structure.[98] For delivery systems that require individual layer scanning times on a similar scale as the breathing motion, optimizing the spot delivery sequence in conjunction with rescanning can maximize the area the beam can cover per time period and mitigate interplay effects.[16]

4.5 | Active motion-management techniques

Active motion-management techniques encompass all approaches in which a deliberate effort is made to modify the patient's breathing pattern (e.g., BH) or modify the actual particle-beam delivery to synchronize with the respiratory pattern (e.g., gating, tracking). Active motion-management strategies usually tend to offer greater benefits when the magnitude of the intrafraction motion is above a certain threshold value. In the context of photon-beam therapy, AAPM Task Group 76[41] proposed a minimum threshold of 5 mm peak-to-peak motion for considering active motion-management strategies. Mori et al.,[105] studied the magnitude of residual motion in heavy charged particle therapy and recommended a threshold level of 4 mm before applying any motion-management approaches. Gelover et al., on the other hand, proposed to use 10-mm tumor motion as a threshold for BH or phase-based gating in a spot scanning proton delivery system. This threshold was applied in the context of passive rescanning for most (non-BH) cases and was modified as warranted based on recalculating the plan on extreme motion phases for evaluation.[25] Recognizing the applicable motion thresholds for particle therapy is highly dependent on the delivery system, delivery modality, and the use of passive motion management techniques such as rescanning, Chang et al. recommended in a PTCOG consensus guideline that each institution establish its acceptable tumor motion criteria based on its motion-management strategy.[34]

4.5.1 | Gating

Respiratory gating typically includes all techniques limiting particle-beam activation to a predetermined portion of the respiratory cycle. An essential feature of all such approaches is the continuous monitoring of the respiration-associated motion of the tumor or an external or internal surrogate during the simulation and treatment delivery processes.

AAPM Task Group 76[41] provides a broader perspective on respiratory motion management in the context of radiotherapy in general and a general understanding of gating as implemented in photon therapy. Early implementation of gated delivery in particle therapy in Japan dates to the late 1980s.[106,107] A more recent publication describes the clinical implementation of gating for proton PBS.[25] The implementation of respiratory gating for a cyclotron-/synchrotron-based particle delivery system substantially differs from a conventional linear accelerator, as for particle-beam delivery, beam extraction is governed by a magnet excitation cycle pattern.

In addition, different particle-beam delivery modalities (i.e., PS or PBS) introduce their own sets of interactions between respiratory cycle parameters and particle-beam delivery parameters. They may require optimization to facilitate efficient and precisely gated particle-beam delivery. For example, in synchrotron-based delivery systems, particles can only be extracted for beam delivery during discrete "spills" governed by a magnet excitation pattern that typically consists of a series of magnet excitation cycles. The magnet excitation cycle can be either fixed or variable. Therefore, synchronizing the respiratory gating duty cycle with the magnet excitation cycle is highly important to the efficiency and precision of respiratory-gated particle delivery.[108,109]

The gating window and residual motion within the gating window are essential topics for gated treatment. In general, a smaller gating window offers less residual motion, thus, sparing more normal tissue. It is also worth noting that a smaller window is less affected by the interplay effect but is less efficient as it requires a longer delivery time. Studies[27,110] showed that the performance of gating and rescanning varied vastly among different systems, and different combinations of gating window and number of rescanning might be suitable for different dose fractionation as the delivery time varies for different motion-management techniques. Therefore, it is important to determine and evaluate system-specific parameters before putting a specific motion-management technique for patient use. However, the evaluation tools may not be commercially available and need to be developed in-house. Motion hysteresis and irregularities are other factors to consider in gating or tracking techniques where continuous respiratory monitoring occurs,[41] especially when surrogates were used to model the tumor motion.[111] With motion hysteresis and irregularities, the residual motion within the gating window can be slightly larger than the intended window size. These effects should be taken into consideration during the determination and evaluation of the gating window.[36] As previously mentioned in Section 4.4.4, PCR could also efficiently mitigate interplay effects in the residual motion.[88,94,95]

4.5.2 | Breath-hold

Another active approach to managing respiratory motion during particle-beam delivery is to "arrest" or contain such motion. Arresting respiratory motion can

be achieved both with (voluntary) and without (involuntary) active cooperation from the patient. Both voluntary and involuntary BH-based approaches have been adequately described in the context of motion management during photon-beam delivery.[112–114] As with BH-based photon therapy, typical factors that influence the success of a BH-based particle therapy approach include the BH position's interbreath variability, the median BH duration, and patient training.

For the BH technique, the total treatment time is of critical importance regardless of the delivery technique. As the treatment time prolongs, the patient may not hold their breath consistently due to fatigue. Therefore, the BH technique has been frequently used with PS delivery because delivery can typically be completed within 1 min. BH is comparatively challenging for use with PBS, primarily because of the energy-switching times and spot-switching times in the case of discrete spot scanning; the delivery time for large tumors can exceed 2 min in the absence of BH. For synchrotron-based PBS, multienergy extraction (which reduces the energy-switching time between layers) may improve the efficacy of this technique.[25]

4.5.3 | Abdominal compression

Abdominal compression (AC) has been used to forcibly limit the extent of target motion by limiting abdominal excursion with a clamp-style device or an inflatable belt. Compared to BH, AC more efficiently mitigates motion magnitude,[115] as it does not require waiting for multiple BH periods or extending the treatment duration. AC is routinely used to reduce treatment margins in PS beam delivery, and its use can be extended to PBS[67] to reduce the interplay effect. With any other active motion-management strategy, the reduction of tumor motion has to be evaluated using image guidance-based motion analysis. AC reduced the extent of target motion but did not eliminate it. Therefore, the usual FB workflow and passive motion-management technique would still be applicable in conjunction with AC. The benefit of the AC approach must also be evaluated against the level of discomfort experienced by the patient from the clamping action during imaging and treatment delivery. AC may not be compatible with patients with colostomy bags or other external medical accessories. Even when applicable, AC is not always better than other approaches in managing interfraction changes, although stereotactic hard AC reduces the magnitude of intrafractional motion.[116] Another specific concern about this approach in the context of particle therapy is the effect of the AC device itself on the penetration of the particle beam. Therefore, the material and shape of the device need to be carefully designed.[117] Volume imaging should be used to ensure the positioning of the AC device remains consistent relative to the target for each treatment. As

with other active motion-management techniques, it is crucial to use imaging techniques to confirm that during treatment, the patient's breathing pattern with AC remains the same as simulation[118] and interfraction reproducibility.[119,120]

4.5.4 | Apneic oxygenation

Apneic oxygenation is an advanced form of BH in which the patient's breathing is stopped for an extended period. This procedure usually involves the use of anesthesia and requires the participation of an anesthesiologist during CT and treatment procedures. It is more commonly used in Europe than in the United States and Asia. A summary of the procedure as used with a modulated scanning proton beam was published by Moyers and Vatnitsky.[81] The nonbreathing period is long enough to perform an entire helical CT or treatment portal. For treatment, breathing is stopped for the entire time needed to deliver one portal, but the patient is ventilated at normal tidal levels between portals. Typically, 10 min of extra room time is required each day per patient for this procedure.

4.5.5 | High-frequency jet ventilation (HFJV) and high-frequency percussive ventilation (HFPV)

High-frequency jet ventilation (HFJV)[121,122] and high-frequency percussive ventilation (HFPV)[123] are methods that mechanically force air into the lungs at greater than 60 breaths per minute but with minimal tidal volumes (40 mL). HFPV is unique because it does not require intubation and sedation; it was well tolerated in volunteers.[123] In a study for stereotactic radiosurgery of liver with X-ray beams,[124] motion was measured to be less than 3 mm using HFJV.

4.5.6 | Tracking

Tracking for particle therapy involves real-time or near real-time adaptation of pencil-beam position and energy changes that result in synchronization of the Bragg peak in response to continual change in the target position.[34] Greater confidence in such estimation of Bragg peak position can be achieved with a real-time 3D model of the patient to account for dynamic changes in WET. An accurate measure of all system latencies between detection of motion and initiation of response to the change in position by the delivery system is essential to optimize the treatment delivery process. Tracking also requires real-time integration of treatment delivery systems with imaging systems and a more intensive commercial or in-house technical support level. While

tracking has been implemented for X-ray therapy, no commercial tracking delivery system for particle therapy is available. Tumor tracking information is currently being used for gated treatment.[125,126]

4.5.7 | Active motion-management techniques for SBRT with particle beams

The use of active motion-management techniques, such as gating and BH, is often desirable in the SBRT setting, especially for particle therapy. There are several considerations to encourage the use of active motion management for SBRT:

1. Active motion management effectively reduces the respiratory motion during beam on compared to FB treatment.
2. As a result of less respiratory motion, active motion management requires less geometric target expansion during treatment planning, thus, implicitly improving normal tissue sparing, which is paramount for SBRT.
3. In consideration of (4D) cumulative dosimetry, motion-interplay effects are less likely to average out.
4. Qualified medical physicist (QMP) is required to be readily available for SBRT treatment delivery.[127] Thus, there exists compatibility with the heightened surveillance needs associated with active motion management.

4.6 | 4D dose and dynamic 4D dose calculation

Nonrigid registration is used to propagate the dose from the individual motion phases to the reference motion phase, typically the end-exhale phase, which is required in accumulating 4DD or D4DD. Therefore, uncertainties in DIR directly, albeit complex, impact the deformed and accumulated dose distribution.[128] The dosimetric impacts became, in general, less substantial when applying multiple-field plans or using rescanning. Substantial variations among DIR methods have also been reported for prostate cancer treatments.[129]

As previously mentioned, D4DD calculation is essential and often applied in scanned particle therapy in particular. The D4DD calculations have been validated[133,134] and thoroughly studied by several groups.[30,130–133] There were also efforts to include biological effects and MC methods.[134] However, the 4DD and D4DD calculations have not been fully implemented in commercial treatment planning systems (TPSs).[98]

New approaches to 4DD and D4DD calculations are also currently being developed.[17,21,22,132,133,135–142] For example, the 4D tool of NIRS (Chiba, Japan) can be integrated into the clinical infrastructure for assessment of ITV (internal target volume) calculation methods[143] or

of the influence of the gating window on the imaging dose[140] (Figure 6). Similarly, rescanning options (e.g., layered vs. VS, PCR) have been investigated using 4DD calculations.[132,136] These studies typically assume a particular temporal delivery pattern based on specific machine characteristics in the D4DD calculation. Apart from these general approaches, D4DD calculation may be helpful to develop individualized treatment planning prospectively. In an experimental setting, D4DD calculation was used for treatment planning for patients undergoing cardiac arrhythmia ablation to optimize the 4D delivery parameters on a case-by-case basis.[144] Once the 4DD/D4DD calculations are fully integrated into commercial TPSs, a prospective approach can be used for each patient to identify the most appropriate motion-mitigation technique. This approach is handy when multiple options (such as rescanning, gating, or FB-ITVs) are available in an individual center. Such an analysis could even include an assessment of uncertainties.[145]

Retrospective D4DD calculation requires temporally correlated log files from the therapy control system and the motion surrogate to match individual beam spots to phases of 4DCT. Such infrastructure is available in centers that have reported successful validation of D4DD calculation packages but are not yet standard in a typical clinic. The feasibility of retrospective D4DD calculation has been demonstrated for preclinical applications[146] and clinical environments (Figure 7).[141] Proof of the feasibility of such approaches has also been shown for photon-beam therapy.[147–149] Thus, widespread use is feasible in principle. One major limitation of retrospective approaches is the assumption that the pretreatment 4DCT is valid during treatment delivery. Several groups, therefore, have worked on modeling a valid 4DCT for the treatment day. The approach developed by PSI (Villigen, Switzerland) relies on long 4DMRI sequences (partially) used to deform a CT into a so-called 4DCT-MRI.[150–152] Other ideas to address this issue include conducting 4DCT phase calculation based on a model established by the planning 4DCT and daily data such as CBCT (to incorporate baseline shifts) and a breathing motion surrogate (to extract phase and amplitude).[153,154] Fassi et al.[153,154] checked the modeled 4DCT against real follow-up CTs and observed variations in particle range of less than 1.9 mm WEPL. Such dose reconstructions extend beyond the 4DD/D4DD framework previously discussed and will be important for adaptive radiation therapy (ART) approaches that quantitatively accumulate the delivered dose during fractionated radiation therapy.

4.7 | Robustness and motion robustness

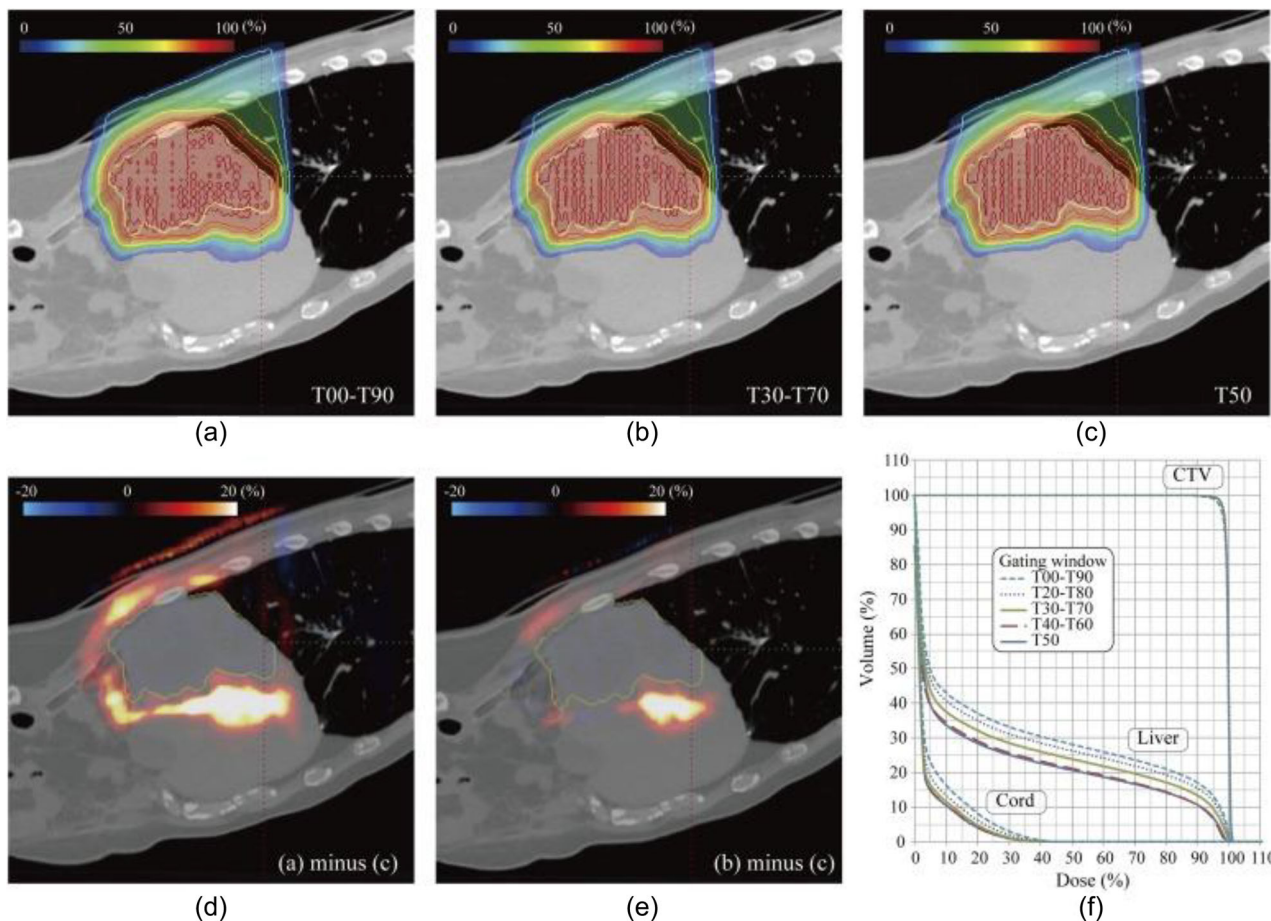A plan's robustness could be quantified by the ability to meet its treatment objectives in the context of

FIGURE 6 4DD accumulation to investigate the influence of the gating window size in treatment of liver cancer with a carbon beam. (a) T00–T90. (b) T30–T70. (c) T50. (d) Panels (a)–(c). (e) Panels (b)–(c). (f) CTV (from Mori S, Karube M, Yasuda S, et al. Gating window dependency on scanned carbon-ion beam dose distribution and imaging dose for thoracoabdominal treatment. Br J Radiol. 2017;90(1074):20160936)
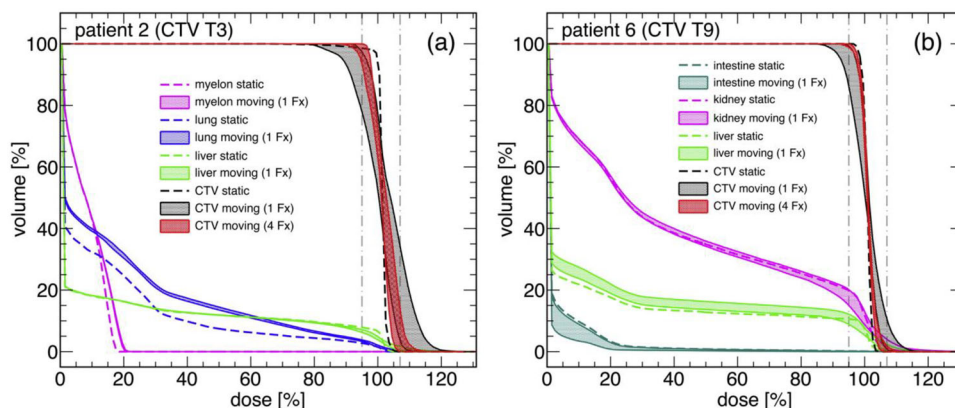

FIGURE 7 Examples of dose reconstruction in hepatocellular carcinoma treatments for a patient treated with abdominal compression (a) and a patient treated with gating (b). (From Richter D, Saito N, Chaudhri N., et al. Four-dimensional patient dose reconstruction for scanned ion beam therapy of moving liver tumors. Int J Radiat Oncol Biol Phys. 2014;89(1):175–181)

given or real uncertainties. Robustness has become an essential concept in particle therapy because particle beams are sensitive to perturbations. A practical method to increase PBS plan robustness is robust optimization,[19,104,155] accounting for uncertainties dur-

ing weight optimization and positioning of spots. Plans are optimized by improving the dose distributions of a number of error scenarios (perturbations) or the worst case among them.[156] Common scenarios include range errors, isocenter shifts, and the use of multiple

CT scans (e.g., to capture breathing phases or multiple time points).[19,155,157–159] Using longitudinal image series may be particularly relevant in the case of anatomic change, and 4D optimization can be considered a special case of robustness optimization using multiple CT scans. Algorithms that include information about the timing of the treatment delivery (i.e., delivery simulation) and a model of patient breathing to create interplay-robust plans are generally in the investigative stage.[160,161] Robust optimization can ensure coverage under given range-calculation uncertainties, setup errors, density variations, and patient anatomy/geometry variations. Its effectiveness is entirely dictated by the appropriate selection of clinically relevant scenarios. Accordingly, the challenge with any robust optimization strategy is not knowing what types of perturbations will be encountered for any given plan or patient.[152,157]

Evaluation of a plan's robustness can also be based on the calculation of perturbed scenarios. While optimization includes a limited number of scenarios, the likelihood of various scenarios can be incorporated into the evaluation by sampling their associated probability distributions.[162] For treatment sites affected by breathing, interplay effect simulations show degradation of dose homogeneity.[27,163] Evaluation of scenario-based dose distributions is commonly based on visualization of dose-volume histogram (DVH) bands encompassing the DVH curves of the individual scenarios,[164] where wider DVH bands usually indicate a less robust plan.[165]

Motion robust evaluation extends the robustness evaluation of setup and range uncertainties to cover respiratory motion. Motion robustness evaluation aims to determine if the treatment plan was acceptable with these uncertainties by using the patient dose distribution with motion uncertainties. However, unlike robust evaluation, which uses population-based range and setup uncertainties, patient-specific images, including simulation 4DCT, repeated CT with BH, or gated CT, are usually used to determine the acceptable degree of robustness to patient motion. For example, the treatment plan can be recalculated on different phases of the 4DCT or the repeat BH CTs. The resulting dose distribution and DVHs can be used for evaluation, which often includes the DVH criteria for the worst-case scenario. This type of static 3D evaluation on multiple CT representations is not sufficient to guarantee robust coverage in the presence of dynamic motion. Still, it can convey important information, such as appropriate target-range coverage or OAR sparing, under specific motion scenarios or breathing states.

4.8 | Image guidance for particle therapy treatment

An extensive review of image guidance in the contemporary particle therapy setting is outside the scope of this report. Paganetti's volume[166] contains a highly relevant chapter on proton image-guided radiation therapy (IGRT); only vital concepts and techniques relevant to motion management will be mentioned here.

IGRT is one of the critical components in modern radiotherapy that facilitates the accurate administration of radiation dose to the patient; it can usually be categorized into (i) initial patient setup, (ii) monitoring during each treatment session (intrafraction), and (iii) monitoring throughout therapy (interfraction), which can be incorporated into plan adaptation. The overarching goal of IGRT is to reproduce the patient anatomy observed at the time of simulation during each treatment session and otherwise minimize or mitigate any observed differences. The initial patient localization/setup tools may be the same or different from those employed for intra- and interfraction monitoring.

4.8.1 | Setup imaging and intrafraction monitoring

The same essential radiographic and tomographic tools used for image guidance in conventional X-ray therapy have also been used for particle therapy. However, some nuanced differences between X-ray and particle therapy image guidance exist, although many similar techniques are used. For example, implementing gantry-mounted CBCT imaging, which has become the mainstream in photon radiotherapy, would not be possible for particle systems with fixed ports.[167] Couch mounted CT, C-arm CT, or CT on rails, while being solutions for volumetric imaging for these systems, may have other drawbacks. For instance, the imaging isocenter may not coincide with the radiation isocenter, which removes the possibility of using them for patient monitoring during treatment.

Fixed-geometry stereoscopic kV imaging systems are gaining more widespread use in particle therapy, particularly in the context of half-gantry or fixed-/multiple-beam port delivery systems. 2D/3D registration has also been deployed in particle therapy, allowing for accurate bony six-degrees-of-freedom registration combined with robotic couches. Such systems can provide fluoroscopic/cine imaging, which could be used as a surrogate patient monitor during treatment.

Optical surface imaging or tracking, which has been steadily gaining traction in the conventional X-ray realm, is also being implemented in particle therapy.[36] When combined with X-ray imaging, optical surface imaging can help to provide a complete picture for initial patient setup and intrafraction monitoring. It has also been used to monitor intrafractional patient motion, including BHs and respiratory gating, for photon and particle therapy.[168] However, current vendor solutions for optical surface imaging may not be comprehensive, especially concerning efficient, built-in workflows, or functions in conjunction with X-ray imaging for motion management.

4.8.2 | Interfraction monitoring and adaptive radiation therapy

Throughout radiation treatment, interfraction change in patient anatomy can be observed using various imaging techniques such as series of 4DCT, daily CBCT images, or fluoroscopy imaging. Typical changes include tumor size, shape, density, weight loss/gain, treatment response, setup variations, and changes in respiratory motion pattern such as variability of amplitude, waveform, the correlation between internal anatomy and external surrogate, and baseline shifts. These changes can be intercorrelated and may not be considered individually in the clinical setting, where a decision needs to be made to proceed with the current plan, or to perform ART considering the dosimetric impact of all the changes observed.

As shown in Figure 8, using weekly serial 4DCT scans, Britton et al. found that gross tumor volume (GTV) trajectories, as represented by the center of mass of the GTV, vary both intrafractional and interfractional for FB NSCLC patients.[169]

Compared to X-ray therapy, charged particle beams can be more sensitive to interfraction changes, and as a result, may need more frequent imaging and more instances of ART.[170,171]

While ART is the current standard approach to address interfraction changes observed during treatment, planning techniques are being investigated to improve the plan's robustness against interfraction changes. Figure 9 shows polar plots of the absolute ΔWEPL calculated for BH CTs acquired at the planning stage and the end of the treatment as a function of the beam angle for all of the patients with right-sided tumors (a-c) and left-sided tumors (d).[69] Similar to intrafractional WEPL analysis, beam angles that minimize ΔWEPL over the entire course of the treatment should be used to improve the robustness of the plan toward interfraction changes, and population studies or prediction based on initial CT may help to optimize beam angle selection. While the current implementation of robustness optimization only considers setup and range uncertainties and not interfraction changes, it was found that robust optimized IMPT plans were more robust toward interfraction changes compared to nonrobust optimized plans.[155] Efforts also exist to explicitly include interfraction changes in the planning process, using the multiple-CT optimization technique, in which plan optimization is performed on multiple CT images simultaneously. Multiple-CT optimization is, to some extent, the natural expansion of robust optimization and 4D optimization, as mentioned in Section 4.7. In addition to the setup and range uncertainties used in robust optimization and the respiratory information used in 4D optimization, multiple-CT optimization applications have used synthetic CTs to account for patient rotation[172]; density overrides such as tumor-density override,[74] gas-

trointestinal tracts gas override; and repeated CT scans performed during treatment.[157] Each approach or strategy was shown to reduce the need for ART during particle therapy treatment.

5 | RECOMMENDATIONS FOR MOTION-ASSESSMENT AND MOTION-MANAGEMENT TECHNIQUES FOR PARTICLE THERAPY

This section summarizes the recommendations from expert consensus within the Task Group for the qualified medical physicist (QMP) (sections 5.1 and 5.2), the radiation oncology department (5.3 and 5.4), and manufacturers (5.5); and provides a sample workflow for motion management in particle therapy (5.6).

5.1 | Recommendations for motion-management programs in particle therapy

5.1.1 | Development of site-specific standard operating procedures and commissioning

Clinical motion management in particle therapy will likely require a unique strategy for each mobile tumor site (or grouping of similar sites). The main driver for motion reduction in conventional X-ray and particle therapy alike is target or irradiated volume reduction. Still, this motivation, reinforced further by motion interplay in particle therapy, must be thoroughly balanced with mathematical rigor, for example, the choice of MC versus analytical algorithms for dose calculation, against treatment efficiency.

This Task Group 290 recommends that, before deployment of motion management for any given or new treatment site, a thorough treatment planning study be performed with retrospective 4DCT data from a representative cohort of patients. Ideally, these patient data would include images collected at multiple time points during the treatment. Users should choose a planning approach that best leverages the available tools, techniques, and beam delivery parameters to devise the best combination (e.g., PS vs. PBS delivery; choice of motion cutoff for phase gating; use of rescanning for PBS; beam spot size selection; and choice of optimization strategy [singlefield, multifield, or robust optimization]). For FB motion-management strategies, 4DD, D4DD, or dose on individual breathing phases should be calculated and evaluated. Importantly, longitudinal 4DCT examinations, if available, can be used to assess the robustness of the various planning techniques over time. Phantom studies can be designed to help validate the conclusions drawn from the 4D calculations depending on the
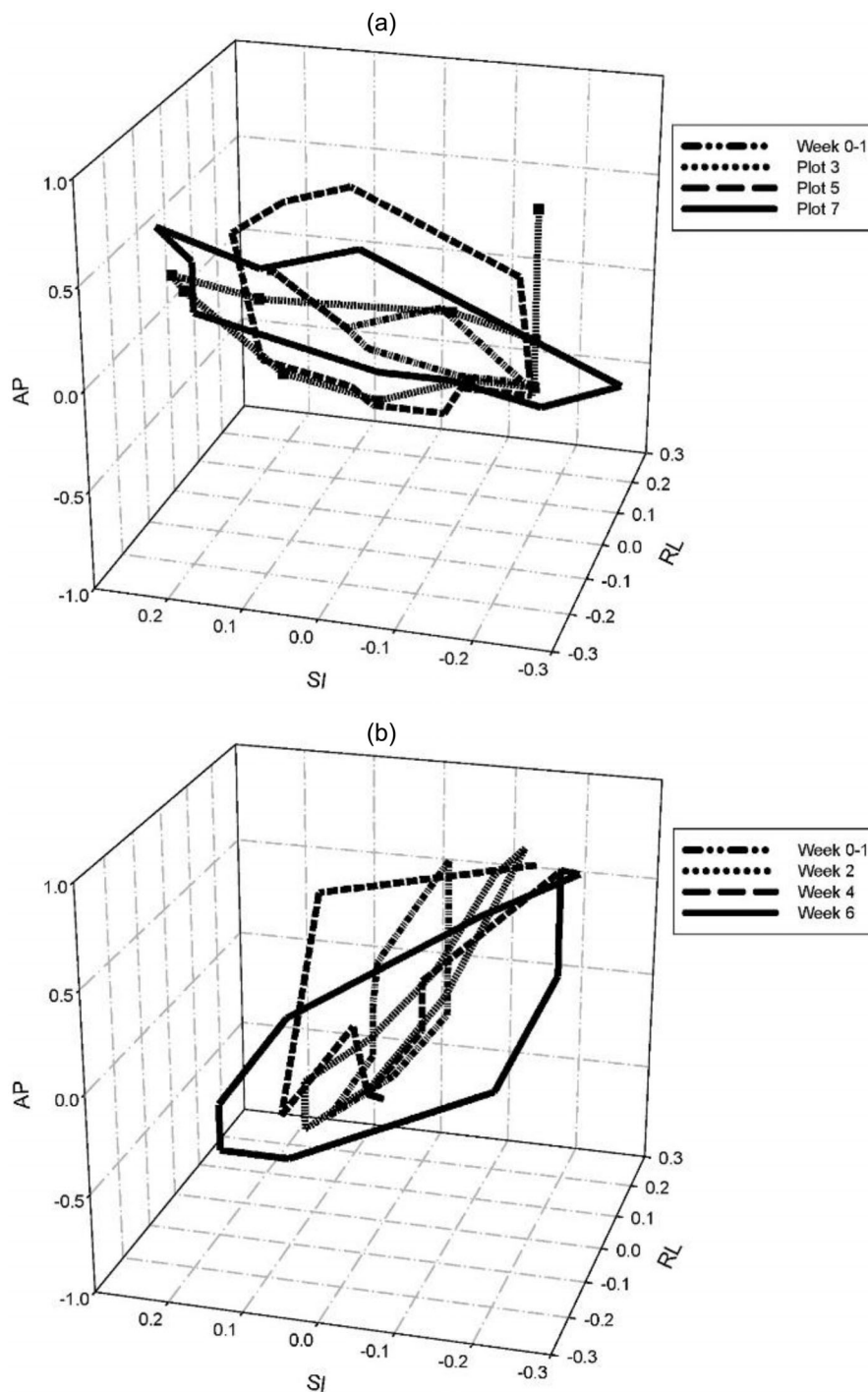
FIGURE 8 Weekly 3D trajectories of the gross tumor volume center of mass during respiration for two patients (Figure 6 from Britton KR, Starkschall G, Tucker SL, et al. Assessment of gross tumor volume regression and motion changes during radiotherapy for non-small-cell lung cancer as measured by four-dimensional computed tomography. Int J Radiat Oncol Biol Phys. 2007;68:1036–1046)

treatment site and availability of representative motion phantoms. If BH treatments are being considered, one of the main concerns is plan robustness to BH variability. Thus, the patient imaging data should include multiple BH scans, ideally obtained with the actual BH technology being considered. If longitudinal BH imaging is not

available, such data could be constructed in silico using deformable techniques.[173]

These planning studies will provide facilities with an informed basis for developing a standard operating procedure (SOP) for a given mobile tumor site. This Task Group recommends that such a site-specific SOP
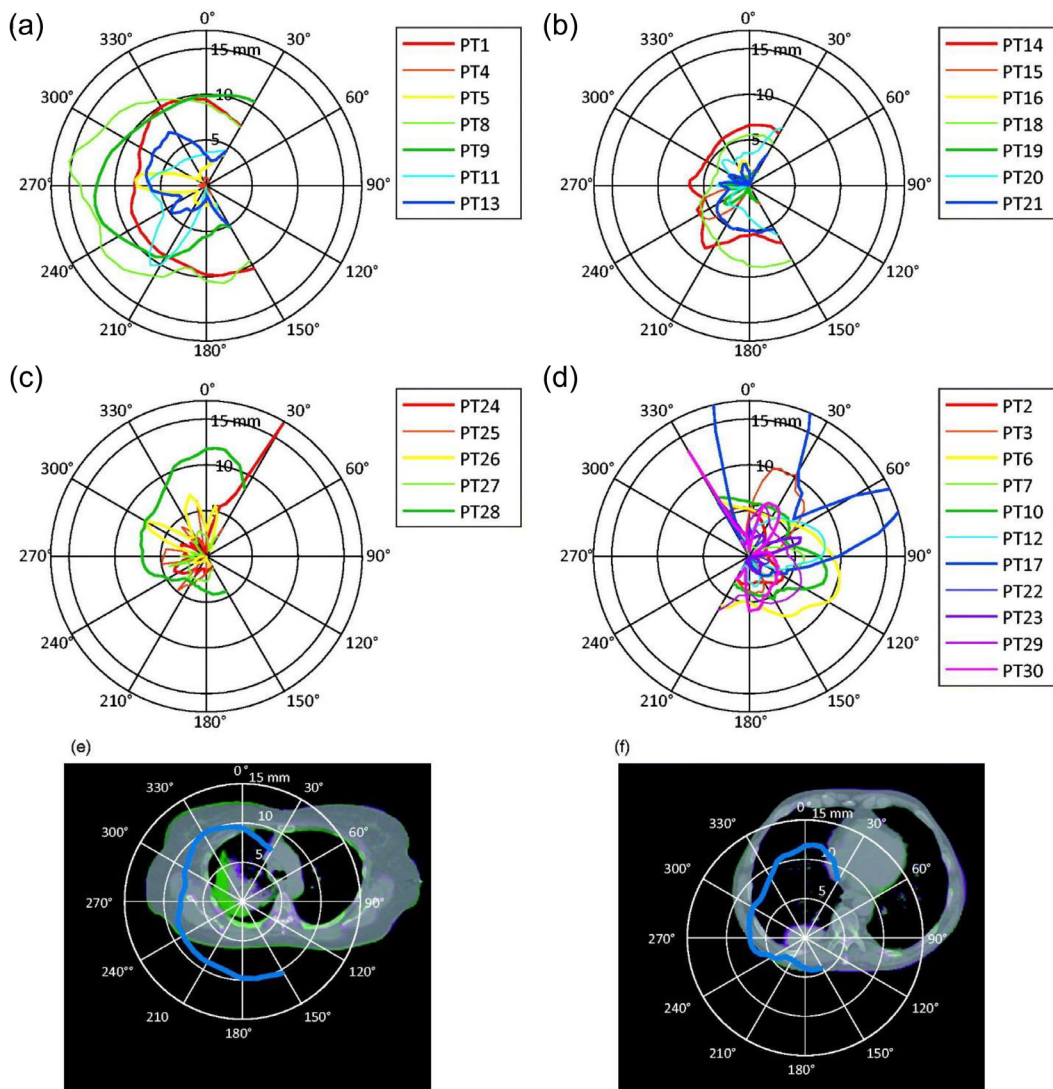
FIGURE 9 Polar plots of the absolute change in water-equivalent path length (ΔWEPL) as a function of beam angle for patients with right-sided tumors (a–c) and left-sided tumors (d), respectively. Patient 17 (PT17) has a maximum ΔWEPL of 41.1 mm (outside the range of the plot). As examples of large WEPL, the polar plots for patients 1 and 28 are overlaid to the image registration in (e, f). Figure 3 from Gorgisyan J, Perrin R, Lomax AJ, et al. Impact of beam angle choice on pencil-beam scanning breath-hold proton therapy for lung lesions. Acta Oncol. 2017;56(6):853-859)

address all aspects of the end-to-end process, from simulation to treatment planning to delivery including IGRT processes.

The SOP should minimally include, when applicable:

· recommendations for patient immobilization;
· description of the simulation imaging required;
· when, who, and how to review the simulation images;
· criteria for any motion-management decisions that need to be made either at the time of simulation (e.g., whether to employ BH) or later in the treatment planning process (e.g., what duty cycle to use for phase gating), and who to make these decisions;
· description of the preferred or standard beam arrangement;

· list and descriptions of structures used for treatment planning and optimization, and any HU, and/or relative linear stopping power (RLSP) overrides;
· beam parameters or parameters used in treatment-plan optimization;
· description of how to perform image guidance with the action thresholds prescribed; and,
· who and how to create documentation for each patient.

SOP development should be tied closely with the commissioning of the motion-management system, which should start with testing individual components as described in the SOP. This approach will ensure each component meets designed or accepted specifications

(examples include the latencies associated with the external surrogate monitoring system, the transfer of gating signals to the planning or delivery systems). Experiments designed to capture or isolate this information should replicate as close as possible the setup that will be employed clinically. Once individual subsystem testing is completed, end-to-end testing (image guidance with dosimetric evaluation) is crucial to assess the overall performance of the motion-management system and the validity of the SOP. The end-to-end test of the SOP should be performed before initial patient treatment and on an annual basis. Depending on the resources available, the SOP could be developed with a limited initial study to establish a set of conservative parameters. The SOP, regardless of the thoroughness of the initial study, should be reviewed and updated after the clinical implementation, as the clinical group gains experience and gains a better understanding of the procedure.

The use of motion phantoms is a critical component in the process described above. Ideally, the phantom should provide a realistic proxy for the moving anatomy, as positioned and treated under image guidance, and a mechanism to measure the dose. 2D film or a 2D matrix of radiation detectors is preferable to a 1D dose measurement because the 2D film provides more complete information, particularly regarding the motion interplay effect. Note that the use of Gafchromic films in the particle therapy context might require an understanding of, or consideration for film "quenching" (or a dependency on linear energy transfer [LET]).[174] The Imaging and Radiation Oncology Core provides a service to dosimetrically measure the end-to-end system performance for motion-managed particle-beam therapy.[175] This Task Group recommends the service or a similar external audit. Such an audit should be treated as a strict requirement if the users cannot complete their internal study of end-to-end motion-management performance.

5.1.2 | Motion assessment

As mentioned previously, 4DCT is the current de facto standard for appropriately representing the motion of an FB target for treatment planning in both particle therapy and X-ray therapy. Initial motion assessments can and should be carried out with the most efficient means available; fluoroscopic or cine X-ray imaging may be more than adequate for making an initial decision at the time of simulation as to whether to perform BH CT or 4DCT simulation. Using X-ray imaging for motion assessment would also reduce the imaging dose to the patient, and pretreatment 4D/cine MRI is also an emerging tool that can be used to assess motion and augment volumetric motion information.

5.1.3 | Treatment planning and evaluation

Treatment planning and evaluation are critically important for a successful motion-management program. However, no commercially available TPS has implemented all the treatment planning and robustness techniques discussed in this report. Therefore, the QMP needs to evaluate how various techniques (or lack thereof) could impact patient care for a particular delivery system. As a minimum, Task Group 290 provides the following recommendations for treatment planning and evaluation.

Beam angle selection
WEPL-based evaluation for individual patients (or to develop a class solution for a particular type of patient) should be used to choose beam angles that minimize ΔWEPL, and therefore, the impact of organ motion. It is worth noting that currently, no commercial TPS allows computation of ΔWEPL. Without such tools, a visual inspection of the 4DCT or multiple BH CTs could still help identify motion robust beam angles. In addition to minimizing ΔWEPL, other factors for beam angle selection, such as minimizing OAR dose, avoiding high LET/relative biological effectiveness dose to OAR,[176] should also be considered.

Application of treatment planning-based techniques
Many motion-management techniques, including target volume override, BSPTV, motion robust optimization, and rescanning, could be implemented in TPS. QMP should be aware of such techniques' availability and effectiveness for the specific delivery system, and apply them as needed for individual patients.

Plan motion robustness evaluation
A system should be developed to evaluate the motion robustness of a developed treatment plan based on the chosen delivery and motion-management technique including evaluation criteria and fall back strategy (e.g., replan or use a different technique for motion management).

5.1.4 | Techniques for PS and US delivery systems

Due to the high frequency of range modulation, the interplay is not considered a major issue for PS delivery systems or US systems with ridge filters. For energy-stacking-based US systems, the interplay effect also needs to be considered. As a result, in terms of motion-management strategies, US and PS systems share similar considerations.

The Task Group recommends focusing mainly on reducing the magnitude of motion and motion-related

proton range uncertainties for US and PS delivery systems. Volume imaging, such as CBCT, should be used to ensure that the motion-mitigation method accurately reproduces the tissues' characteristics that the beams pass through.

Beam angles optimization should be to reduce the motion-related treatment margin on the distal side. However, as the OAR at the proximal side can receive a higher dose with PS delivery than with PBS, the choice of a PS system's beam angle can be limited.

5.1.5 | Techniques for PBS delivery systems

This Task Group recommends investigating the clinical feasibility of rescanning to mitigate interplay effects, particularly when treating FB patients with PBS, before exploring more sophisticated motion-management techniques.

Rescanning

The selection of an appropriate rescanning technique at a given institution should consider hardware parameters and treatment planning software compatibility. Simple dosimetry measurements with 1D, 2D, or 3D dynamic motion phantoms and an ion chamber array or film should be performed to explore the available rescanning parameter space including tumor size, depth, shape, motion range, and the number of rescans. Further, dosimetric commissioning measurements should be taken with static phantom geometries to demonstrate dosimetric equivalence of a set of test plans with and without rescanning (for equivalent total MU per field), and the capacity of improvement of rescanning with dynamic phantom geometries. Institution-specific tolerances on dosimetric equivalence should be established partly based on machine and delivery specifications.

A cutoff motion range, below which interplay may be neglected, should also be determined by taking the following parameters into account: tumor size, depth, shape, motion range, and the number of rescans. Based on surveys shown in Supporting information Table S1 and published literature,[177] a conservative estimation of the cutoff motion range, for example, 5 mm, could be used in the absence of data to complete the study to derive the cutoff range.

Besides evaluating the dosimetric effectiveness of rescanning, clinical delivery efficiency is also an important parameter to consider when selecting a rescanning technique, especially in the context of a multi-room facility, where the patient waiting time while on the treatment table may increase setup uncertainties and decrease patient throughput. D4DD could provide insight into these considerations.

Dynamic 4DD calculations (or similar dynamic simulations)

This Task Group sees D4DD as a vital tool in motion management. Where D4DD calculations are available, the best practice is to use the site- and case-specific timing information. The timing information typically cannot be directly deduced from published studies because the timing depends on the institution's specific PBS configuration, such as required number of rescans, effective spot size, spot spacing, minimum deliverable MU, spot delivery technique and sequence, energy-switching time, in-layer spot delivery timings, and the potential for real-time spot delivery synchronization with patients' breathing. D4DD calculations rely heavily on the accuracy of a site-specific spot delivery timing model[178] and the accuracy of DIR. This Task Group, thus, recommends that each site validates the D4DD calculations with phantom measurements as well.

5.2 | Recommendations for active motion-management techniques

As mentioned in Section 4.5, active motion management techniques require varying levels of additional involvement and support from both the patient and the treatment team to achieve the overarching goal of reducing target motion uncertainty during beam delivery.

5.2.1 | Recommendations for selection of active motion-management techniques

Figure 10 illustrates a qualitative comparison of various active motion-management techniques currently being explored or used for/during particle-beam delivery for their staff and patient training, delivery variables, and commercial support requirements. In Figure 10, the active motion-management techniques are scored for each evaluation metric on the vertical axis using a numerical scale on the horizontal axis that reflects its relative importance. In general, active motion-management techniques require a moderate-to- high level of patient involvement. BH usually requires the highest level of patient coaching and practice to yield the best results. In contrast, apneic oxygenation needs no patient training and a high level of anesthesiology support (non-RO staff requirement). Patient compliance with breathing regularity or BH length usually has some impact on the quality of the treatment. Requirements and availability for commercial and in-house technical support, including implementation, validation, commissioning, and patient and equipment QA needs, along with staff training, both within Radiation Oncology departments and complementary clinical care teams (such as nursing, anesthesiology), will also need to be evaluated thoroughly before

FIGURE 10 An example of qualitative comparison of active motion-management techniques currently proposed for implementation during particle therapy. The required participation or the effect of active motion-management techniques (tracking, apneic oxygenation, abdominal compression, breath-hold, respiratory gating) were estimated for each of the evaluation metrics using a numerical scale (1 to 5 [highest])

settling on appropriate active motion-management techniques. A robust triage process is also essential to identify the appropriate motion-management technique for each patient.

It has to be reiterated that while numerous techniques described above are available, not all of them may apply to the given facility. There exists a strong dependence on compatibility with the given facility's IGRT capabilities. Furthermore, it is likely the case that no singular approach will serve all patients' needs. Hence, depending upon the level of technical and personnel support available, multiple techniques should be considered for adoption, to be used either in isolation or used in combination. Each facility can develop a qualitative evaluation process similar to Figure 10 to help in prioritizing the implementation process. The appropriate motion-management technique for a given patient should be decided with a team approach involving a radiation oncologist, QMP, and therapist, to enhance patient compliance, satisfaction, and overall treatment delivery accuracy.

5.2.2 | Recommendations for implementation of specific active motion-management techniques

In addition to recommendations in section 5.1.1, before patient use, the effects of residual motion, including baseline shifts within the respiratory gate or BH, should also be thoroughly evaluated and well documented by a QMP. The interplay effect of the residual motion should be assessed for the given delivery system for scanning beam delivery. Mitigation strategies, such as reducing gating window, rescanning, or breath sampling rescanning should be considered. In general, fast delivery is desirable for BH delivery for BH consistency. As discussed in Section 4.5.1, some of these evaluations may not be feasible with commercially available tools and may need in-house development.

For individual patients, the duration of each gate cycle/BH and the reproducibility of target position between breath cycles or BHs should be evaluated by assessing repeat imaging at simulation before treatment planning and confirmed using pretreatment imaging before treatment delivery. When applicable, proper consideration should be given to the typical beam pulsed delivery duty cycles (cyclotron and synchrotron systems) and synchronizing with the actual patient respiratory cycles or BHs. In addition, patient compliance with any active BH facilitator (such as active breathing control or AC) should be determined at simulation.

5.3 | Recommendations on image guidance, equipment, and clinical decision-making

It is essential to recognize that, although the technologies used in particle therapy for IGRT are similar to those used in conventional external-beam therapy, the implementation of IGRT in the clinical process must be different for particle therapy because of the sensitivity of dose deposition to anatomy and ΔWEPL. Thus, this

Task Group recommends that a QMP review and discuss the following aspects for particle therapy with team members in the radiation oncology department:

1. QMP should be familiar with the functionality, accuracy, and specifications of the implemented imaging technologies, and understand the dosimetric impact of the uncertainties resulting from the IGRT procedure, ideally, for individual patients.
2. QMP should have a thorough understanding of the interaction between the imaging and delivery system, which is particularly important for patient treatments with active motion management.
3. IGRT clinical decision-making schemes for motion management in particle therapy must be thoroughly considered on a per-site basis, with a clear identification of roles and responsibilities of each team member. These schemes will likely vary from those used in X-ray therapy and will also vary with the motion-management strategy employed.

5.4 | Recommendations on repeated imaging during treatment

As discussed in Section 4.8.2., the degree of interfraction change of patient motion varies, and the sensitivity of the dose distribution toward the interfraction change might depend on treatment planning and delivery techniques. Therefore, a conservative plan to monitor the robustness of the dose distribution by performing volumetric CT imaging with a specific frequency (e.g., weekly) is prudent, especially when facilities have less experience treating the applicable site, or without on-board volumatric imaging.

5.5 | Recommendations for manufacturers

5.5.1 | Communication and information sharing

Many commercial and home-made devices are available to assist the user with motion management during the planning and delivery of external-beam radiation therapy. These devices typically need to be synchronized with the imaging and beam delivery systems. Thus, providing safe and effective treatment requires accurate data transmission between the imaging, treatment planning, and delivery systems. Therefore, this Task Group recommends that both health care organizations and vendors join the Integrating Healthcare Enterprise-Radiation Oncology (IHE-RO) initiative that aims to improve system-to-system connections and, thus, helps to ensure a safe, efficient radiation oncology practice.

Both users and manufacturers of equipment used for patient motion management will find documents published by the International Electrotechnical Commission (IEC) and DICOM helpful in establishing a standard communication framework in the broad context of radiotherapy, and more specifically, motion management. For example, the DICOM communication standard already includes some elements on motion management, but these are seldom used in TPSs, beam delivery systems, or motion-management equipment. To improve the safety and accuracy of treatments, manufacturers should strive to incorporate standard methods of communicating motion-management information between various pieces of equipment. Our specific recommendations include:

· Incorporating transmission of motion parameters, including waveforms from motion sensors and/or image systems (e.g., 4DCT) to the TPS.
· Incorporating transmission of motion parameters from the TPS to the delivery system.
· Displaying the motion parameters used during treatment (e.g., waveform, gating parameters) at the treatment console during setup.
· Incorporating the patient motion parameters during delivery into the existing scanning beam delivery record enables the association of breathing and scanning beam delivery.

5.5.2 | Imaging and image guidance

Given the importance of image guidance in particle therapy and accurate modeling of the patient for motion management, this Task Group recommends that manufacturers implement the following to improve imaging and image guidance:

· Improve imaging capacity for image guidance. Examples include improving in-room volumetric imaging to enable 4D (CB)CT, BH (CB)CT, or (4D/BH) MRI, and improving real-time imaging of the patient.
· Improve the integration of imaging and delivery systems to enable active motion-management techniques such as gating. For example, the ability to image within the same logical "gate" used for treatment, or image at a certain point in the respiratory cycle, is often lacking.
· Improve image guidance workflow to enable fast dose calculation/validation and online adaptation using in-room imaging.

5.5.3 | 4DD and D4DD calculation

As detailed in Section 4.6, 4DD and D4DD calculations are essential in implementing PBS for moving targets. Therefore, this Task Group recommends that
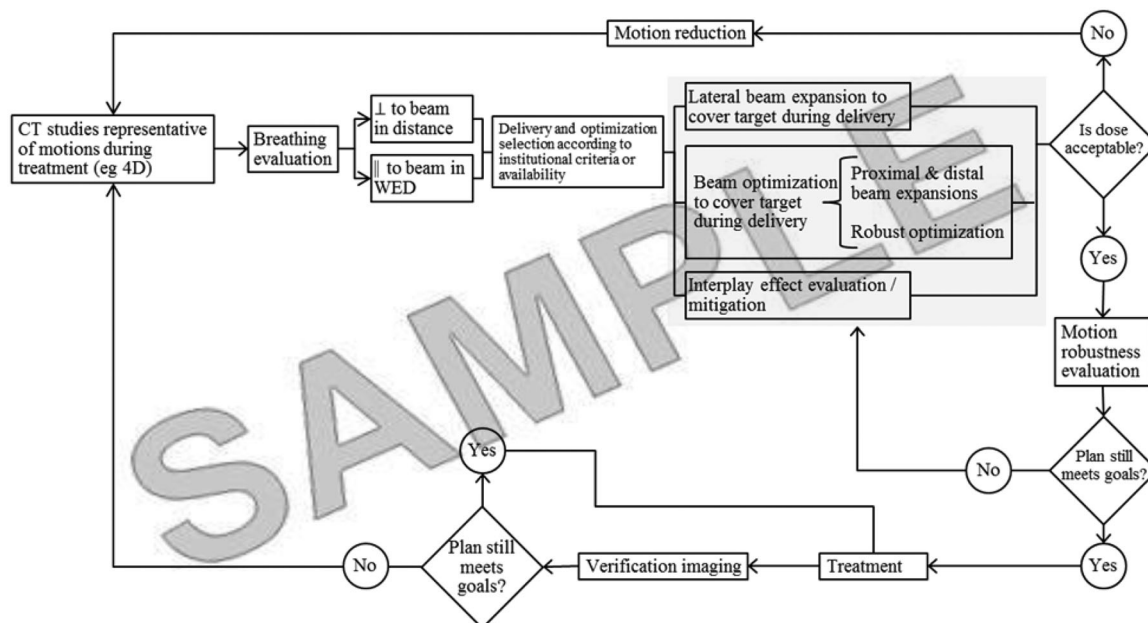
FIGURE 11　Sample workflow for motion management in particle therapy. *WED water-equivalent depth, a synonym of WEPL

manufacturers support 4DD and D4DD calculations in their TPSs. In addition to the information and communication issues mentioned above, our specific recommendations include:

· Incorporate DIR, automatic contour propagation, and dose deformation into the treatment planning workflow.
· Enable beam angle-specific WEPL (ΔWEPL) analysis.
· Enable 4D optimization. Manufacturers should also extend the concepts of robust optimization and 4D optimization to allow for additional freedom in terms of plan optimization such as multiple-CT optimization.

5.6 | Sample workflow

Figure 11 shows a sample workflow for motion management in particle therapy. For example, the figure illustrates the crucial steps of motion evaluation (both perpendicular and parallel to the beam direction), the decision on whether to use motion-reduction techniques, interplay evaluation, motion robustness evaluation, and verification imaging. Specific criteria should be developed for each of these steps using the characteristics of the TPS and treatment delivery system.

6 | RISK FACTORS AND RISK MITIGATION IN THE CLINICAL DEPLOYMENT OF MOTION-MANAGEMENT STRATEGIES FOR PARTICLE THERAPY

With an increasing consensus about the need to manage the quality and safety based on the weaknesses

and vulnerabilities in the complex workflow or processes of radiotherapy, our field has begun adopting prospective quality management (QM) techniques, such as failure modes and effects analysis (FMEA), as opposed to reactive QM. While conventional photon radiotherapy benefits from a high degree of standardization in equipment, procedures, and quality control protocols for motion management, particle therapy shows a wide variation in adapting a mitigation strategy which is also continuously evolving with advancements in the technology. This broad range of strategies requires a higher degree of customization in the QM than those with intimate knowledge of the specific strategies must be carried out.

To facilitate the development of a prospective QM program, an FMEA analysis was performed for the process of treating a moving target with particle therapy. The identified risk factors are summarized and discussed in this section. TG-290 shares the experts' opinions on relevant risk factors and potential mitigations so that they are not neglected but instead incorporated in a site-specific analysis performed in individual clinics. The presented analysis focuses on the identification of risk factors only. However, it does not address the design of potential quality improvement programs or interventions that will lower the overall risk score for each failure mode, an essential aspect of a complete FMEA-base QM when performed by a specific clinic. The analysis was carried out by the task group members, a total of six QMPs who are actively involved in the adaptation and management of motion-management strategies in their clinic. The motion-management process for particle radiotherapy follows a similar sequence of processes associated with conventional radiotherapy, as illustrated in the generic IMRT process of TG-100.[179] Still, it

TABLE 1 Summary of FMEA analysis listing failure modes with the highest 20% average RPN (≥250) and relatively high average severity scores (Avg. S ≥ 7)

Stage in Workflow	Failure Mode	Potential Cause	Motion Management Technique	Modality	Occurrence	Severity	Detection	RPN
A. Motion modeling	Error in the delineation of ITV and GTV	Unstable or irregular breathing	*	*	6.3	6.7	5.0	251
	Target delineated for a wrong CT phase (or image)	Human error	*	*	5.8	6.8	5.5	237
	Target delineated for a wrong CT phase (or image)	Misguided BH instruction	BH	*	4.8	7.5	5.5	223
	Target delineated for a wrong CT phase (or image)	The wrong phases/duty cycle selected for gating	FB-Gating	*	5.3	7.7	5.8	251
B. Planning	Error in hardware fabrication	The wrong volume was chosen for aperture fabrication		*	4.5	7.8	5.8	185
	Dose calculated on a wrong CT phase (or image)	Human error		*	4.9	7.0	4.7	170
	Dose calculated on a wrong CT phase (or image)	BH or AC scan accidentally used for FB/Gating or vice versa		*	4.2	7.5	5.3	167
	Error in range computed for a beam	Plan not cast on extreme motion phases of 4D-CT as a check on range robustness	FB-ITV, FB-4D	*	4.7	7.0	5.0	178
C. Localization	Target missed	X-ray imaging unavailable or not used for setup	*	*	5.2	7.5	4.7	138
	Target missed	Lack of standard protocol	FB-Gating, BH	*	5.9	6.5	5.2	270
	Target missed	Human error	FB-Gating, BH	*	6.0	6.8	5.5	260
D. Tx delivery	Error in dose delivered or target not covered	Large baseline shift (during treatment after imaging)	*	*	5.2	6.5	6.2	236
	"	Motion amplitude different from simulation	FB-ITV, FB-Gating, FB-4D	*	6.3	5.7	6.8	269
	"	Breath-hold baseline drifted due to patient fatigue	BH	*	6.5	6.8	5.8	279
	Large interplay effects	The residual motion of the target is too large	FB-Gating, AC, BH	PBS	6.3	6.5	5.8	279
	Beam not held for gated/BH treatments	Plan not properly configured (DICOM) for "gating"	FB-Gating, BH	*	5.3	6.7	5.0	248

Abbreviations. AC, abdominal compression; BH, Breath-hold; FB, free-breathing; GTV, gross tumor volume; ITV, internal target volume.
Note that, for each of the FMEA metrics, values averaged over all respondents are shown.

features additional steps in CT simulation, treatment planning, localization, and treatment delivery. These steps are needed to; (a) model and assess the extent of the motion; (b) proactively account for the motion in planning; and (c) set up and treat the moving target. For this analysis, the workflow shown in Figure 11 was used as a sample process map.

Only motion-management strategies that are widely practiced were considered in the process. They are FB-ITV, FB-gating, FB with robust optimization using 4D CT (FB-4D), motion-suppressed AC, and BH. Three treatment delivery modalities currently in practice, that is, PS, US, and PBS are included. However, in the context of failure modes in motion management, PS and US are not uniquely different and are, therefore, considered together in the analysis. Similarly, the technical differences in delivering pencil spots in PBS (e.g., raster vs. spot scanning) were considered indiscernible. The analyzed failure modes are specific only to motion-management strategies, and a deliberate effort was made to reduce redundant failure modes with the conventional treatments of static targets.

Potential causes of failure modes (a total of 50) were generated in discussions with inputs from the group. They are attributed to (a) *patient factors* including patient compliance; anatomy motion outside of the target; interplay effect with beam delivery; and changes in motion pattern or magnitude during a treatment course; (b) *equipment factors* including limitations in imaging and motion assessment; synchronization with beam delivery (lagging); synchronization with patient motion; beam delivery uncertainties; and (c) *human factors* including documentation and training related risks. Risk assessments were based on three attributes scored on a 10-point scale: severity if the failure occurs, S; probability of occurrence of this particular failure, O; and the probability that this particular failure would go undetected, D. The interpretations of the 10-point scales are semiquantitative but explicitly followed the TG-100 scales in the assessment. For each failure mode, the risk priority numbers (RPN defined as the product of S, O, and D) were computed and then averaged over all the respondents. The failure modes were ranked in order of importance using the averaged RPNs. An RPN score conceptually represents the risk posed to the patient by undetected failures.

6.1 | Summary of FMEA analysis

Failure modes with the associated RPN values are categorized by mitigation strategies and treatment modalities and summarized in Table 1. Average RPN values ranged from 57 to 279. Failure modes having the highest-ranked 20% (determined to be high-risk) are listed in the table. No failure mode was identified to show the average severity above nine (i.e., possible severe toxicity or tumor underdose, or catastrophic), while the average values ranged from 4.7 to 7.8. Failure modes causing relatively high severity (i.e., S $\geq$ 7) are also listed in the table for reference.

It is noticeable that those surveyed found that the treatment delivery process poses the most high-risk failure modes. The high risks are attributed to uncertainties in breathing patterns. When active motion-management strategies, such as FB-gating, AC, or BH are used, the risk increases with the added complexity of procedures. Therefore, the corresponding QM should be elevated with appropriate staff training and standardized procedures. Moreover, if the residual motion is large and unaccounted for even when active mitigation strategies are used for treating a moving target, the target coverage could still be compromised due to interplay effects, which is one failure mode specific to PBS, as noted in the table.

7 | SUMMARY

This Task Group recommends that before deployment of motion management for any treatment site, a thorough, well-documented treatment planning study is performed using retrospective 3D or 4D CT data from a representative cohort of patients. Based on the findings of this study, an SOP for the mobile tumor site should be developed. The Task Group recommends that this site-specific SOP address all aspects of the process, from simulation to treatment delivery including image-guidance processes. The SOP should *minimally* include recommendations for patient immobilization; a description of the simulation imaging required; when, who, and how to review the simulation images; criteria for any motion-management decisions that need to be made either at the time of simulation (e.g., whether to employ BH) or later in the treatment planning process (e.g., what duty cycle to use for phase gating), and who to make these decisions; description of the preferred or standard beam arrangement; list and descriptions of structures used for treatment planning and optimization, and any HU and/or RLSP overrides; beam parameters or parameters used in treatment-plan optimization; a description of how to perform image guidance with the action thresholds prescribed; and, who and how to create documentation for each patient. An end-to-end test of the SOP should be performed before initial patient treatment and annually. A risk-based methodology should be adopted to establish the QM program and as an ongoing activity aimed toward continuous process improvement.

Flampouri, Kyung-Wook Jee, Liyong Lin, Michael Moyers, Shinichiro Mori, Joerg Rottmann, Erik Tryggestad, Sastry Vedam.

REFERENCES

1. Chang JY, Li H, Zhu XR, et al. Clinical implementation of intensity modulated proton therapy for thoracic malignancies. *Int J Radiat Oncol Biol Phys*. 2014; 90(4): 809–818.

2. Zhang X, Li Y, Pan X, et al. Intensity-modulated proton therapy reduces the dose to normal tissue compared with intensity-modulated radiation therapy or passive scattering proton therapy and enables individualized radical radiotherapy for extensive stage IIIB non-small-cell lung cancer: a virtual clinical study. *Int J Radiat Oncol Biol Phys*. 2010; 77(2): 357–366.

3. Wang X, Krishnan S, Zhang X, et al. Proton radiotherapy for liver tumors: dosimetric advantages over photon plans. *Med Dosim*. 2008; 33(4): 259–267.

4. Doyen J, Falk AT, Floquet V, Hérault J, Hannoun-Lévi J-M. Proton beams in cancer treatments: clinical outcomes and dosimetric comparisons with photon therapy. *Cancer Treat Rev*. 2016; 43: 104–112.

5. Engelsman M, Schwarz M, Dong L. Physics controversies in proton therapy. *Semin Radiat Oncol*. 2013;23(2):88–96.

6. Phillips MH, Pedroni E, Blattmann H, Boehringer T, Coray A, Scheib S. Effects of respiratory motion on dose uniformity with a charged particle scanning method. *Phys Med Biol*. 1992; 37(1): 223–234.

7. Bert C, Durante M. Motion in radiotherapy: particle therapy. *Phys Med Biol*. 2011; 56(16): R113–144.

8. Tryggestad EJ, Liu W, Pepin MD, Hallemeier CL, Sio TT. Managing treatment-related uncertainties in proton beam radiotherapy for gastrointestinal cancers. *J Gastrointest Oncol*. 2020; 11(1): 212–224.

9. Kraus KM, Heath E, Oelfke U. Dosimetric consequences of tumour motion due to respiration for a scanned proton beam. *Phys Med Biol*. 2011; 56(20): 6563–6581.

10. Lambert J, Suchowerska N, McKenzie DR, Jackson M. Intrafractional motion during proton beam scanning. *Phys Med Biol*. 2005; 50(20): 4853–4862.

11. Seco J, Robertson D, Trofimov A, Paganetti H. Breathing interplay effects during proton beam scanning: simulation and statistical analysis. *Phys Med Biol*. 2009; 54(14): N283–294.

12. Bert C, Grozinger SO, Rietzel E. Quantification of interplay effects of scanned particle beams and moving targets. *Phys Med Biol*. 2008; 53(9): 2253–2265.

13. Knopf A, Bert C, Heath E, et al. Special report: workshop on 4D-treatment planning in actively scanned particle therapy—Recommendations, technical challenges, and future research directions. *Med Phys*. 2010; 37(9): 4608–4614.

14. Matney J, Park PC, Bluett J, et al. Effects of respiratory motion on passively scattered proton therapy versus intensity modulated photon therapy for stage III lung cancer: are proton plans more sensitive to breathing motion? *Int J Radiat Oncol Biol Phys*. 2013; 87(3): 576–582.

15. Nohadani O, Seco J, Bortfeld T. Motion management with phase-adapted 4D-optimization. *Phys Med Biol*. 2010; 55(17): 5189.

16. Li H, Zhu XR, Zhang X. Reducing dose uncertainty for spot-scanning proton beam therapy of moving tumors by optimizing the spot delivery sequence. *Int J Radiat Oncol Biol Phys*. 2015; 93(3): 547–556.

17. Kardar L, Li Y, Li X, et al. Evaluation and mitigation of the interplay effects of intensity modulated proton therapy for lung cancer in a clinical setting. *Pract Radiat Oncol*. 2014; 4(6): e259–268.

18. Graeff C. Motion mitigation in scanned ion beam therapy through 4D-optimization. *Phys Med*. 2014; 30(5): 570–577.

19. Liu W, Schild SE, Chang JY, et al. Exploratory study of 4D versus 3D robust optimization in intensity modulated proton therapy for lung cancer. *Int J Radiat Oncol Biol Phys*. 2016; 95(1): 523–533.

20. Schatti A, Zakova M, Meer D, Lomax AJ. Experimental verification of motion mitigation of discrete proton spot scanning by re-scanning. *Phys Med Biol*. 2013; 58(23): 8555–8572.

21. Li Y, Kardar L, Li X, et al. On the interplay effects with proton scanning beams in stage III lung cancer. *Med Phys*. 2014; 41(2): 021721.

22. Knopf AC, Hong TS, Lomax A. Scanned proton radiotherapy for mobile targets-the effectiveness of re-scanning in the context of different treatment planning approaches and for different motion characteristics. *Phys Med Biol*. 2011; 56(22): 7257–7271.

23. Grassberger C, Dowdell S, Lomax A, et al. Motion interplay as a function of patient parameters and spot size in spot scanning proton therapy for lung cancer. *Int J Radiat Oncol Biol Phys*. 2013; 86(2): 380–386.

24. Andersson KM, Edvardsson A, Hall A, Enmark M, Kristensen I. Pencil beam scanning proton therapy of Hodgkin's lymphoma in deep inspiration breath-hold: a case series report. *Tech Innov Patient Support Radiat Oncol*. 2020; 13: 6–10.

25. Gelover E, Deisher AJ, Herman MG, Johnson JE, Kruse JJ, Tryggestad EJ. Clinical implementation of respiratory-gated spot-scanning proton therapy: an efficiency analysis of active motion management. *J Appl Clin Med Phys*. 2019; 20(5): 99–108.

26. Riboldi M, Orecchia R, Baroni G. Real-time tumour tracking in particle therapy: technological developments and future perspectives. *Lancet Oncol*. 2012; 13(9): e383–391.

27. Zhang Y, Huth I, Weber DC, Lomax AJ. A statistical comparison of motion mitigation performances and robustness of various pencil beam scanned proton systems for liver tumour treatments. *Radiother Oncol*. 2018; 128(1): 182–188.

28. ICRU. ICRU Report 78: Prescribing, Recording, and Reporting Proton-Beam Therapy 2007.

29. Das IJ, Paganetti H, Medicine AAoPi. *Principles and practice of proton beam therapy*. Medical Physics Publishing; 2015.

30. Santanam L, Hurkmans C, Mutic S, et al. Standardizing naming conventions in radiation oncology. *Int J Radiat Oncol Biol Phys*. 2012; 83(4): 1344–1349.

31. Mayo CS, Moran JM, Bosch W, et al. American Association of Physicists in Medicine Task Group 263: standardizing nomenclatures in radiation oncology. *Int J Radiat Oncol Biol Phys*. 2018;100(4):1057–1066.

32. Yock AD, Mohan R, Flampouri S, et al. Robustness analysis for external beam radiation therapy treatment plans: describing uncertainty scenarios and reporting their dosimetric consequences. *Pract Radiat Oncol*. 2019; 9(4): 200–207.

33. Khamfongkhruea C, Thongsawad S, Tannanonta C, Chamchod S. Comparison of CT images with average intensity projection, free breathing, and mid-ventilation for dose calculation in lung cancer. *J Appl Clin Med Physics*. 2017; 18(2): 26–36.

34. Chang JY, Zhang X, Knopf A, et al. Consensus guidelines for implementing pencil-beam scanning proton therapy for thoracic malignancies on behalf of the PTCOG thoracic and lymphoma subcommittee. *Int J Radiat Oncol Biol Phys*. 2017; 99(1): 41–50.

35. Li H, Li Y, Zhang X, et al. Dynamically accumulated dose and 4D accumulated dose for moving tumors. *Med Phys*. 2012; 39(12): 7359–7367.

36. Zhang Y, Huth I, Wegner M, Weber DC, Lomax AJ. Surface as a motion surrogate for gated re-scanned pencil beam proton therapy. *Phys Med Biol*. 2017; 62(10): 4046–4061.

37. Mori S, Zenklusen S, Inaniwa T, et al. Conformity and robustness of gated rescanned carbon ion pencil beam scanning of liver tumors at NIRS. *Radiother Oncol*. 2014;111(3):431–436.

38. Rosu M, Hugo GD. Advances in 4D radiation therapy for managing respiration: part II—4D treatment planning. *Z Med Phys*. 2012; 22(4): 272–280.

39. Haberer T, Becher W, Schardt D, Kraft G. Magnetic scanning system for heavy ion therapy. *Nucl Instrum Methods Phys Res A*. 1993;330(1-2):296–305.

40. Zenklusen S, Pedroni E, Meer D. A study on repainting strategies for treating moderately moving targets with proton pencil beam scanning at the new Gantry 2 at PSI. *Phys Med Biol*. 2010; 55(17): 5103.

41. Keall PJ, Mageras GS, Balter JM, et al. The management a of respiratory motion in radiation oncology report of AAPM Task Group 76. *Med Phys*. 2006; 33(10): 3874–3900.

42. Ford E, Mageras G, Yorke E, Ling C. Respiration-correlated spiral CT: method of measuring respiratory-induced anatomic motion for radiation treatment planning. *Medcial Physics*. 2003; 30(1): 88–97.

43. Yu ZH, Lin SH, Balter P, Zhang L, Dong L. A comparison of tumor motion characteristics between early stage and locally advanced stage lung cancers. *Radiother Oncol*. 2012; 104(1): 33–38.

44. Shimizu S, Shirato H, Xo B, et al. Three-dimensional movement of a liver tumor detected by high-speed magnetic resonance imaging. *Radiother Oncol*. 1999; 50(3): 367–370.

45. Lever FM, Lips IM, Crijns SP, et al. Quantification of esophageal tumor motion on cine-magnetic resonance imaging. *Int J Radiat Oncol Biol Phys*. 2014; 88(2): 419–424.

46. von Siebenthal M, Szekely G, Gamper U, Boesiger P, Lomax A, Cattin P. 4D MR imaging of respiratory organ motion and its variability. *Phys Med Biol*. 2007; 52(6): 1547–1564.

47. Kirilova A, Lockwood G, Choi P, et al. Three-dimensional motion of liver tumors using cine-magnetic resonance imaging. *Int J Radiat Oncol Biol Phys*. 2008; 71(4): 1189–1195.

48. Hallman JL, Mori S, Sharp GC, Lu HM, Hong TS, Chen GT. A four-dimensional computed tomography analysis of multiorgan abdominal motion. *Int J Radiat Oncol Biol Phys*. 2012; 83(1): 435–441.

49. Tai A, Liang Z, Erickson B, Li XA. Management of respiration-induced motion with 4-dimensional computed tomography (4DCT) for pancreas irradiation. *Int J Radiat Oncol Biol Phys*. 2013; 86(5): 908–913.

50. Zhao KL, Liao Z, Bucci MK, et al. Evaluation of respiratory-induced target motion for esophageal tumors at the gastroesophageal junction. *Radiother Oncol*. 2007; 84(3): 283–289.

51. Park JC, Park SH, Kim JH, et al. Liver motion during cone beam computed tomography guided stereotactic body radiation therapy. *Med Phys*. 2012; 39(10): 6431–6442.

52. Nishioka T, Nishioka S, Kawahara M, et al. Synchronous monitoring of external/internal respiratory motion: validity of respiration-gated radiotherapy for liver tumors. *Jpn J Radiol*. 2009; 27(7): 285–289.

53. Abbas H, Chang B, Chen ZJ. Motion management in gastrointestinal cancers. *J Gastrointest Oncol*. 2014; 5(3): 223–235.

54. Mori S, Dong L, Starkschall G, Mohan R, Chen GT. A serial 4DCT study to quantify range variations in charged particle radiotherapy of thoracic cancers. *J Radiat Res*. 2014; 55(2): 309–319.

55. Bortfeld T, Jokivarsi K, Goitein M, Kung J, Jiang SB. Effects of intra-fraction motion on IMRT dose delivery: statistical analysis and simulation. *Phys Med Biol*. 2002; 47(13): 2203–2220.

56. Yu CX, Jaffray DA, Wong JW. The effects of intra-fraction organ motion on the delivery of dynamic intensity modulation. *Phys Med Biol*. 1998; 43(1): 91.

57. Bortfeld T, Jiang SB, Rietzel E. Effects of motion on the total dose distribution. Paper presented at: Seminars in radiation oncology 2004.

58. Dowdell S, Grassberger C, Sharp GC, Paganetti H. Interplay effects in proton scanning for lung: a 4D Monte Carlo study assessing the impact of tumor and beam delivery parameters. *Phys Med Biol*. 2013; 58(12): 4137–4156.

59. Taylor PA, Kry SF. Followill DS. Pencil beam algorithms are unsuitable for proton dose calculations in lung. *Int J Radiat Oncol* Biol* Phys*. 2017; 99(3): 750–756.

60. Kang M, Huang S, Solberg TD, et al. A study of the beam-specific interplay effect in proton pencil beam scanning delivery in lung cancer. *Acta Oncol (Madr)*. 2017; 56(4): 531–540.

61. Huang S, Souris K, Li S, et al. Validation and application of a fast Monte Carlo algorithm for assessing the clinical impact of approximations in analytical dose calculations for pencil beam scanning proton therapy. *Med Phys*. 2018; 45(12): 5631–5642.

62. Koybasi O, Mishra P, James SS, Lewis JH, Seco J. Simulation of dosimetric consequences of 4D-CT-based motion margin estimation for proton radiotherapy using patient tumor motion data. *Phys Med Biol*. 2014; 59(4): 853.

63. James SS, Mishra P, Hacker F, Berbeco RI, Lewis JH. Quantifying ITV instabilities arising from 4DCT: a simulation study using patient data. *Phys Med Biol*. 2012; 57(5): L1.

64. De Ruysscher D, Faivre-Finn C, Nestle U, et al. European Organisation for Research and Treatment of Cancer recommendations for planning and delivery of high-dose, high-precision radiotherapy for lung cancer. *J Clin Oncol*. 2010; 28(36): 5301–5310.

65. Brandner ED, Chetty IJ, Giaddui TG, Xiao Y, Huq MS. Motion management strategies and technical issues associated with stereotactic body radiotherapy of thoracic and upper abdominal tumors: a review from NRG oncology. *Med Phys*. 2017;44(6):2595–2612.

66. Casares-Magaz O, Toftegaard J, Muren LP, et al. A method for selection of beam angles robust to intra-fractional motion in proton therapy of lung cancer. *Acta Oncol (Madr)*. 2014; 53(8): 1058–1063.

67. Lin L, Souris K, Kang M, et al. Evaluation of motion mitigation using abdominal compression in the clinical implementation of pencil beam scanning proton therapy of liver tumors. *Med Phys*. 2017; 44(2): 703–712.

68. Yu J, Zhang X, Liao L, et al. Motion-robust intensity-modulated proton therapy for distal esophageal cancer. *Med Phys*. 2016; 43(3): 1111–1118.

69. Gorgisyan J, Perrin R, Lomax AJ, et al. Impact of beam angle choice on pencil beam scanning breath-hold proton therapy for lung lesions. *Acta Oncol*. 2017; 56(6): 853–859.

70. Siddon RL. Fast calculation of the exact radiological path for a three-dimensional CT array. *Med Phys*. 1985; 12(2): 252–255.

71. Fukumoto S. Cyclotron versus synchrotron for proton beam therapy. 14th International Conference on Cyclotrons and their Applications, 1995; Cape Town, South Africa.

72. Schippers JM, Cyclotrons for Particle Therapy *arXiv preprint arXiv:180408541*. 2018. Presented at the CAS- CERN Accelerator School on Accelerators for Medical Application, Vösendorf, Austria.

73. James SS, Grassberger C, Lu H-M. Considerations when treating lung cancer with passive scatter or active scanning proton therapy. *Transl Lung Cancer Res*. 2018; 7(2): 210–215.

74. Kang Y, Zhang X, Chang JY, et al. 4D Proton treatment planning strategy for mobile lung tumors. *Int J Radiat Oncol Biol Phys*. 2007; 67(3): 906–914.

75. Urie M, Goitein M, Wagner M. Compensating for heterogeneities in proton radiation therapy. *Phys Med Biol*. 1984; 29(5): 553–566.

76. Moyers MF, Miller DW, Bush DA, Slater JD. Methodologies and tools for proton beam design for lung tumors. *Int J Radiat Oncol Biol Phys*. 2001; 49(5): 1429–1438.

77. Farr J, Mascia A, Hsi WC, et al. Clinical characterization of a proton beam continuous uniform scanning system with dose layer stacking. 2008; 35(11): 4945–4954.

78. Nichiporov D, Hsi W, Farr JJMp. Beam characteristics in two different proton uniform scanning systems: a side-by-side comparison. 2012; 39(5): 2559–2568.

79. Larsson B, Leksell L, Rexed B, Sourander P. Effect of high energy protons on the spinal cord. *Acta Radiol*. 1959; 51(1): 52–64.

80. Ertan E, Muller-Sievers K, Riehl G. A new approach to overcome the inconveniences in electron dosimetry associated with the beam scanning technique in linacs. *Phys Med Biol*. 1984; 29(7): 789–796.

81. Moyers MF, Vatnitsky SM. Practical implementation of light ion beam treatments. *Med Phys*. 2014;41:017302.

82. Kanai T, Kawachi K, Kumamoto Y, et al. Spot scanning system for proton radiotherapy. *Med Phys*. 1980; 7(4): 365–369.

83. Pedroni E, Bacher R, Blattmann H, et al. Cancer therapy with 200 MeV protons at PSI. Development of a fast beam scanning method and future plans for a hospital based facility. Paper presented at: 2nd European Particle Accelerator Conference; 12–6 June 1990, Nice, France.

84. Haberer T, Becher W, Schardt D, Kraft G. Magnetic scanning system for heavy-ion therapy. *Nucl Instrum Methods Phys Res A: Accel Spectrom Detect Assoc Equip*. 1993; 330(1-2): 296–305.

85. Zenklusen SM, Pedroni E, Meer D. A study on repainting strategies for treating moderately moving targets with proton pencil beam scanning at the new Gantry 2 at PSI. *Phys Med Biol*. 2010; 55(17): 5103–5121.

86. Kohno R, Hotta K, Dohmae T, et al. Development of continuous line scanning system prototype for proton beam therapy. *Int J Particl Therap*. 2017; 3(4): 429–438.

87. Kang JH, Wilkens JJ, Oelfke U. Demonstration of scan path optimization in proton therapy. *Med Phys*. 2007; 34(9): 3457–3464.

88. Furukawa T, Inaniwa T, Sato S, et al. Design study of a raster scanning system for moving target irradiation in heavy-ion radiotherapy. *Med Phys*. 2007; 34(3): 1085–1097.

89. Klimpki G, Zhang Y, Fattori G, et al. The impact of pencil beam scanning techniques on the effectiveness and efficiency of rescanning moving targets. *Phys Med Biol*. 2018; 63(14): 145006.

90. Schätti A, Meer D, Lomax AJPiM. Biology. First experimental results of motion mitigation by continuous line scanning of protons. *Phys Med Biol*. 2014; 59(19): 5707.

91. Park PC, Zhu XR, Lee AK, et al. A beam-specific planning target volume (PTV) design for proton therapy to account for setup and range uncertainties. *Int J Radiat Oncol Biol Phys*. 2012; 82(2): e329-e336.

92. Rietzel E, Bert C. Respiratory motion management in particle therapy. *Med Phys*. 2010; 37(2): 449–460.

93. Poulsen PR, Eley J, Langner U, Simone CB 2nd, Langen K. Efficient interplay effect mitigation for proton pencil beam scanning by spot-adapted layered repainting evenly spread out over the full breathing cycle. *Int J Radiat Oncol Biol Phys*. 2018; 100(1): 226–234.

94. Furukawa T, Inaniwa T, Sato S, et al. Moving target irradiation with fast rescanning and gating in particle therapy. *Med Phys*. 2010;37(9):4874–4879.

95. Mori S, Furukawa T, Inaniwa T, et al. Systematic evaluation of four-dimensional hybrid depth scanning for carbon-ion lung therapy. *Med Phys*. 2013; 40(3): 031720.

96. Protik A, van Herk M, Witte M, Sonke J-J. The impact of breathing amplitude on dose homogeneity in intensity modulated proton therapy. *Phys Imag Radiat Oncol*. 2017; 3: 11–16.

97. van de Water S, Safai S, Schippers JM, Weber DC, Lomax AJ. Towards FLASH proton therapy: the impact of treatment planning and machine characteristics on achievable dose rates. *Acta Oncol*. 2019; 58(10): 1463–1469.

98. Engwall E, Glimelius L, Hynning E. Effectiveness of different rescanning techniques for scanned proton radiotherapy in lung cancer patients. *Phys Med Biol*. 2018; 63(9): 095006.

99. Li H, Zhang X, Li Y, Zhu RX. An analytical model for the upper bound estimation of respiratory motion–induced dose uncertainty in spot-scanning proton beam therapy. *Med Phys*. 2019; 46(11): 5249–5261.

100. Liu C, Schild SE, Chang JY, et al. Impact of spot size and spacing on the quality of robustly optimized intensity modulated proton therapy plans for lung cancer. *Intl J Radiat Oncol*Biol*Phys*. 2018;101(2):479–489.

101. Kraan AC, Depauw N, Clasie B, Giunta M, Madden T, Kooy HM. Effects of spot parameters in pencil beam scanning treatment planning. *Med Phys*. 2018; 45(1): 60–73.

102. Oelfke U, Bortfeld T. Inverse planning for photon and proton beams. *Med Dosi*. 2001; 26(2): 113–124.

103. Unkelbach J, Bortfeld T, Martin BC, Soukup M. Reducing the sensitivity of IMPT treatment plans to setup errors and range uncertainties via probabilistic treatment planning. *Med Phys*. 2009; 36(1): 149–163.

104. Liu W, Zhang X, Li Y, Mohan R. Robust optimization of intensity modulated proton therapy. *Med Phys*. 2012; 39(2): 1079–1091.

105. Mori S, Asakura H, Kandatsu S, Kumagai M, Baba M, Endo M. Magnitude of residual internal anatomy motion on heavy charged particle dose distribution in respiratory gated lung therapy. *Int J Radiat Oncol Biol Phys*. 2008; 71(2): 587–594.

106. Minohara S, Kanai T, Endo M, Noda K, Kanazawa M. Respiratory gated irradiation system for heavy-ion radiotherapy. *Int J Radiat Oncol Biol Phys*. 2000; 47(4): 1097–1103.

107. Ohara K, Okumura T, Akisada M, et al. Irradiation synchronized with respiration gate. *Int J Radiat Oncol Biol Phys*. 1989; 17(4): 853–857.

108. Tsunashima Y, Vedam S, Dong L, et al. Efficiency of respiratory-gated delivery of synchrotron-based pulsed proton irradiation. *Phys Med Biol*. 2008; 53(7): 1947–1959.

109. Tsunashima Y, Vedam S, Dong L, Umezawa M, Balter P, Mohan R. The precision of respiratory-gated delivery of synchrotron-based pulsed beam proton therapy. *Phys Med Biol*. 2010; 55(24): 7633–7647.

110. Bert C, Gemmel A, Saito N, Rietzel E. Gated irradiation with scanned particle beams. *Int J Radiat Oncol Biol Phys*. 2009; 73(4): 1270–1275.

111. Ruan D, Fessler JA, Balter J, Berbeco R, Nishioka S, Shirato H. Inference of hysteretic respiratory tumor motion from external surrogates: a state augmentation approach. *Phys Med Biol*. 2008; 53(11): 2923.

112. Hoppe BS, Mendenhall NP, Louis D, Li Z, Flampouri S. Comparing breath hold and free breathing during intensity-modulated radiation therapy and proton therapy in patients with mediastinal Hodgkin lymphoma. *Int J Particl Therap*. 2017; 3(4): 492–496.

113. Yu J, Park SS, Herman MG, Langen K, Mehta M, Feigenberg SJ. Free breathing versus breath-hold scanning beam proton therapy and cardiac sparing in breast cancer. *Int J Particl Therap*. 2016; 3(3): 407–413.

114. Dueck J, Knopf AC, Lomax A, et al. Robustness of the voluntary breath-hold approach for the treatment of peripheral lung tumors using hypofractionated pencil beam scanning proton therapy.. *Int J Radiat Oncol Biol Phys*. 2016;95(1):534–541.

115. Eccles CL, Patel R, Simeonov AK, Lockwood G, Haider M, Dawson LA. Comparison of liver tumor motion with and without abdominal compression using cine-magnetic resonance imaging. *Int J Radiat Oncol Biol Phys*. 2011; 79(2): 602–608.

116. Bengua G, Ishikawa M, Sutherland K, et al. Evaluation of the effectiveness of the stereotactic body frame in reducing respiratory intrafractional organ motion using the real-time tumor-tracking radiotherapy system. *Int J Radiat Oncol Biol Phys*. 2010; 77(2): 630–636.

117. Dolde K, Schneider S, Stefanowicz S, et al. comparison of pancreatic respiratory motion management with three abdominal corsets for particle radiation therapy: case study. *J Appl Clin Med Phys*. 2019; 20(6): 111–119.

118. Habermehl D, Debus J, Ganten T, et al. Hypofractionated carbon ion therapy delivered with scanned ion beams for patients with hepatocellular carcinoma–feasibility and clinical response. *Radiat Oncol.* 2013; 8(1): 59.

119. Lee M, Simeonov A, Stanescu T, Dawson LA, Brock KK, Velec M. MRI evaluation of normal tissue deformation and breathing motion under an abdominal compression device. *J Appl Clin Med Phys.* 2021; 22(2): 90–97.

120. Eccles CL, Dawson LA, Moseley JL, Brock KK. Interfraction liver shape variability and impact on GTV position during liver stereotactic radiotherapy using abdominal compression. *Int J Radiat Oncol* Biol* Phys.* 2011; 80(3): 938–946.

121. Santiago A, Jelen U, Ammazzalorso F, et al. Reproducibility of target coverage in stereotactic spot scanning proton lung irradiation under high frequency jet ventilation. *Radiother Oncol.* 2013; 109(1): 45–50.

122. Santiago A, Fritz P, Mühlnickel W, Engenhart-Cabillic R, Wittig A. Changes in the radiological depth correlate with dosimetric deterioration in particle therapy for stage I NSCLC patients under high frequency jet ventilation. *Acta Oncol.* 2015; 54(9): 1631–1637.

123. Sala IM, Nair GB, Maurer B, MGuerrero T. High frequency percussive ventilation for respiratory immobilization in radiotherapy. *Tech Innovat Patient Supp Radiat Oncol.* 2019; 9: 8–12.

124. Fritz P, Kraus H-J, Dölken W, Mühlnickel W, Müller-Nolte F, Hering W. Gold marker implants and high-frequency jet ventilation for stereotactic, single-dose irradiation of liver tumors. *Technol in Cancer Res Treat.* 2006; 5(1): 9–14.

125. Shibata S, Takamatsu S, Yamamoto K, et al. Proton beam therapy without fiducial markers using four-dimensional CT planning for large hepatocellular carcinomas. *Cancers (Basel).* 2018; 10(3):71.

126. Shimizu S, Miyamoto N, Matsuura T, et al. A proton beam therapy system dedicated to spot-scanning increases accuracy with moving tumors by real-time imaging and gating and reduces equipment size. *PLoS One.* 2014; 9(4): e94971.

127. Chao ST, Dad LK, Dawson LA, et al. ACR-ASTRO practice parameter for the performance of stereotactic body radiation therapy. *Am J Clin Oncol.* 2020; 43(8): 545–552.

128. Ribeiro CO, Knopf A, Langendijk JA, Weber DC, Lomax AJ, Zhang Y. Assessment of dosimetric errors induced by deformable image registration methods in 4D pencil beam scanned proton treatment planning for liver tumours. *Radiother Oncol.* 2018; 128(1): 174–181.

129. Abe Y, Kadoya N, Arai K, et al. Effect of DIR uncertainty on prostate passive-scattering proton therapy dose accumulation. *Phys Med.* 2017; 39: 113–120.

130. Bert C, Richter D, Durante M, Rietzel E. Scanned carbon beam irradiation of moving films: comparison of measured and calculated response. *Radiat Oncol.* 2012; 7: 55.

131. Richter D, Schwarzkopf A, Trautmann J, et al. Upgrade and benchmarking of a 4D treatment planning system for scanned ion beam therapy. *Med Phys.* 2013; 40(5): 051722.

132. Takahashi W, Mori S, Nakajima M, et al. Carbon-ion scanning lung treatment planning with respiratory-gated phase-controlled rescanning: simulation study using 4-dimensional CT data. *Radiat Oncol.* 2014; 9: 238.

133. Zhang Y, Boye D, Tanner C, Lomax AJ, Knopf A. Respiratory liver motion estimation and its effect on scanned proton beam therapy. *Phys Med Biol.* 2012; 57(7): 1779–1795.

134. Grassberger C, Daartz J, Dowdell S, Ruggieri T, Sharp G, Paganetti H. Quantification of proton dose calculation accuracy in the lung. *Int J Radiat Oncol Biol Phys.* 2014; 89(2): 424–430.

135. Batista V, Richter D, Combs SE, Jakel O. Planning strategies for inter-fractional robustness in pancreatic patients treated with scanned carbon therapy. *Radiat Oncol.* 2017; 12(1): 94.

136. Bernatowicz K, Lomax AJ, Knopf A. Comparative study of layered and volumetric rescanning for different scanning speeds of proton beam in liver patients. *Phys Med Biol.* 2013; 58(22): 7905–7920.

137. Grassberger C, Dowdell S, Sharp G, Paganetti H. Motion mitigation for lung cancer patients treated with active scanning proton therapy. *Med Phys.* 2015; 42(5): 2462–2469.

138. Jakobi A, Perrin R, Knopf A, Richter C. Feasibility of proton pencil beam scanning treatment of free-breathing lung cancer patients. *Acta Oncol.* 2018; 57(2): 203–210.

139. Mori S, Inaniwa T, Furukawa T, et al. Amplitude-based gated phase-controlled rescanning in carbon-ion scanning beam treatment planning under irregular breathing conditions using lung and liver 4DCTs. *J Radiat Res.* 2014; 55(5): 948–958.

140. Mori S, Karube M, Yasuda S, Yamamoto N, Tsuji H, Kamada T. Gating window dependency on scanned carbon-ion beam dose distribution and imaging dose for thoracoabdominal treatment. *Br J Radiol.* 2017; 90(1074): 20160936.

141. Richter D, Graeff C, Jakel O, Combs SE, Durante M, Bert C. Residual motion mitigation in scanned carbon ion beam therapy of liver tumors using enlarged pencil beam overlap. *Radiother Oncol.* 2014; 113(2): 290–295.

142. Wolfelschneider J, Friedrich T, Luchtenborg R, et al. Impact of fractionation and number of fields on dose homogeneity for intra-fractionally moving lung tumors using scanned carbon ion treatment. *Radiother Oncol.* 2016; 118(3): 498–503.

143. Mori S, Inaniwa T, Miki K, Shirai T, Noda K. Implementation of a target volume design function for intrafractional range variation in a particle beam treatment planning system. *Br J Radiol.* 2014; 87(1043): 20140233.

144. Lehmann HI, Graeff C, Simoniello P, et al. Feasibility study on cardiac arrhythmia ablation using high-energy heavy ion beams. *Sci Rep.* 2016;6:38895.

145. Hild S, Durante M, Bert C. Assessment of uncertainties in treatment planning for scanned ion beam therapy of moving tumors. *Int J Radiat Oncol Biol Phys.* 2013; 85(2): 528–535.

146. Richter D, Lehmann HI, Eichhorn A, et al. ECG-based 4D-dose reconstruction of cardiac arrhythmia ablation with carbon ion beams: application in a porcine model. *Phys Med Biol.* 2017; 62(17): 6869–6883.

147. Kamerling CP, Fast MF, Ziegenhein P, Menten MJ, Nill S, Oelfke U. Real-time 4D dose reconstruction for tracked dynamic MLC deliveries for lung SBRT. *Med Phys.* 2016;43(11):6072.

148. Imae T, Haga A, Saotome N, et al. Dose reconstruction using respiratory signals and machine parameters during treatment in stereotactic body radiotherapy. *Nihon Hoshasen Gijutsu Gakkai Zasshi.* 2014; 70(11): 1225–1234.

149. Ravkilde T, Skouboe S, Hansen R, Worm E, Poulsen PR. First online real-time evaluation of motion-induced 4D dose errors during radiotherapy delivery. *Med Phys.* 2018; 45(8): 3893–3903.

150. Bernatowicz K, Peroni M, Perrin R, Weber DC, Lomax A. Four-dimensional dose reconstruction for scanned proton therapy using liver 4DCT-MRI. *Int J Radiat Oncol Biol Phys.* 2016; 95(1): 216–223.

151. Boye D, Lomax T, Knopf A. Mapping motion from 4D-MRI to 3D-CT for use in 4D dose calculations: a technical feasibility study. *Med Phys.* 2013; 40(6): 061702.

152. Dolde K, Naumann P, David C, et al. 4D dose calculation for pencil beam scanning proton therapy of pancreatic cancer using repeated 4DMRI datasets. *Phys Med Biol.* 2018; 63(16): 165005.

153. Wolfelschneider J, Seregni M, Fassi A, et al. Examination of a deformable motion model for respiratory movements and 4D dose calculations using different driving surrogates. *Med Phys.* 2017; 44(6): 2066–2076.

154. Fassi A, Seregni M, Riboldi M, et al. Surrogate-driven deformable motion model for organ motion tracking in particle radiation therapy. *Phys Med Biol.* 2015; 60(4): 1565–1582.

155. Li H, Zhang X, Park P, et al. Robust optimization in intensity-modulated proton therapy to account for anatomy changes in lung cancer patients. *Radiother Oncol.* 2015; 114(3): 367–372.

156. Unkelbach J, Paganetti H. Robust proton treatment planning: physical and biological optimization. *Semin Radiat Oncol*. 2018; 28(2): 88–96.

157. Wang X, Li H, Zhu XR, et al. Multiple-CT optimization of intensity-modulated proton therapy - Is it possible to eliminate adaptive planning? *Radiother Oncol*. 2018; 128(1): 167–173.

158. Liu W, Liao Z, Schild SE, et al. Impact of respiratory motion on worst-case scenario optimized intensity modulated proton therapy for lung cancers. *Pract Radiat Oncol*. 2015; 5(2): e77-e86.

159. Ma J, Wan Chan Tseung HS, Herman MG, Beltran C. A robust intensity modulated proton therapy optimizer based on Monte Carlo dose calculation. *Med Phys*. 2018; 45(9): 4045–4054.

160. Engwall E, Fredriksson A, Glimelius L. 4D robust optimization including uncertainties in time structures can reduce the interplay effect in proton pencil beam scanning radiation therapy. *Med Phys*. 2018; 45(9): 4020–4029.

161. Pepin MD, Tryggestad E, Wan Chan Tseung HS, Johnson JE, Herman MG, Beltran C. A Monte-Carlo-based and GPU-accelerated 4D-dose calculator for a pencil beam scanning proton therapy system. *Med Phys*. 2018; 45(11): 5293–5304.

162. van der Voort S, van de Water S, Perko Z, Heijmen B, Lathouwers D, Hoogeman M. Robustness recipes for minimax robust optimization in intensity modulated proton therapy for oropharyngeal cancer patients. *Int J Radiat Oncol Biol Phys*. 2016; 95(1): 163–170.

163. Inoue T, Widder J, van Dijk LV, et al. Limited impact of setup and range uncertainties, breathing motion, and interplay effects in robustly optimized intensity modulated proton therapy for stage III non-small cell lung cancer. *Int J Radiat Oncol Biol Phys*. 2016; 96(3): 661–669.

164. Trofimov A, Unkelbach J, DeLaney TF, Bortfeld T. Visualization of a variety of possible dosimetric outcomes in radiation therapy using dose-volume histogram bands. *Pract Radiat Oncol*. 2012; 2(3): 164–171.

165. Shan J, An Y, Bues M, Schild SE, Liu W. Robust optimization in IMPT using quadratic objective functions to account for the minimum MU constraint. *Med Phys*. 2018; 45(1): 460–469.

166. Paganetti H. *Proton therapy physics*. CRC press; 2018.

167. Landry G, Hua CH. Current state and future applications of radiological image guidance for particle therapy. *Med Phys*. 2018; 45(11): e1086-e1095.

168. Patel SA, Lu H-M, Nyamwanda JA, et al. Postmastectomy radiation therapy technique and cardiopulmonary sparing: a dosimetric comparative analysis between photons and protons with free breathing versus deep inspiration breath hold. 2017; 7(6): e377-e384.

169. Britton KR, Starkschall G, Tucker SL, et al. Assessment of gross tumor volume regression and motion changes during radiotherapy for non-small-cell lung cancer as measured by four-dimensional computed tomography. *Int J Radiat Oncol Biol Phys*. 2007; 68: 1036–1046.

170. Yang P, Xu T, Gomez DR, et al. Patterns of local-regional failure after intensity modulated radiation therapy or passive scattering proton therapy with concurrent chemotherapy for non-small cell lung cancer. *Int J Radiat Oncol Biol Phys*. 2019; 103(1): 123–131.

171. Chen M, Yang J, Liao Z, et al. Anatomic change over the course of treatment for non–small cell lung cancer patients and its impact on intensity-modulated radiation therapy and passive-scattering proton therapy deliveries. *Radiat Oncol*. 2020; 15(1): 1–11.

172. Tang S, Song L, Sturgeon JD, Chang C. Robust planning for a patient treated in decubitus position with proton pencil beam scanning radiotherapy. *Cureus*. 2017; 9(9).

173. den Otter LA, Kaza E, Kierkels RG, et al. Reproducibility of the lung anatomy under active breathing coordinator control: dosimetric consequences for scanned proton treatments. *Med Phys*. 2018; 45(12): 5525–5534.

174. Reinhardt S, Hillbrand M, Wilkens JJ, Assmann W. Comparison of Gafchromic EBT2 and EBT3 films for clinical photon and proton beams. *Med Phys*. 2012; 39(8): 5257–5262.

175. Taylor PA, Kry SF, Alvarez P, et al. Results from the imaging and radiation oncology core houston's anthropomorphic phantoms used for proton therapy clinical trial credentialing. *Int J Radiat Oncol Biol Phys*. 2016; 95(1): 242–248.

176. Paganetti H, Blakely E, Carabe-Fernandez A, et al. Report of the AAPM TG-256 on the relative biological effectiveness of proton beams in radiation therapy. *Med Phys*. 2019; 46(3): e53-e78.

177. Mori S, Knopf AC, Umegaki K. Motion management in particle therapy. *Med Phys*. 2018; 45(11): e994-e1010.

178. Shen J, Tryggestad E, Younkin JE, et al. Using experimentally determined proton spot scanning timing parameters to accurately model beam delivery time. *Med Phys*. 2017; 44(10): 5081–5088.

179. Huq MS, Fraass BA, Dunscombe PB, et al. The report of Task Group 100 of the AAPM: application of risk analysis methods to radiation therapy quality management. *Med Phys*. 2016; 43(7): 4209–4262.

180. Graeff C, Bert C. Noninvasive cardiac arrhythmia ablation with particle beams. *Med Phys*. 2018; 45(11): e1024-e1035.

181. Fuster V, Ryden LE, Cannom DS, et al. ACCF/AHA/HRS focused updates incorporated into the ACC/AHA/ESC 2006 Guidelines for the management of patients with atrial fibrillation: a report of the American College of Cardiology Foundation/American Heart Association Task Force on Practice Guidelines developed in partnership with the European Society of Cardiology and in collaboration with the European Heart Rhythm Association and the Heart Rhythm Society. *J Am Coll Cardiol*. 2011;57(11):e101–198.

182. Cronin EM, Bogun FM, Maury P, et al. HRS/EHRA/APHRS/LAHRS expert consensus statement on catheter ablation of ventricular arrhythmias. *J Interv Card Electrophysiol*. 2020;59:145–298. https://doi.org/10.1007/s10840-019-00663-3.

183. Guerra PG, Talajic M, Thibault B, et al. Beta-radiation for the creation of linear lesions in the canine atrium. *Circulation*. 2004; 110(8): 911–914.

184. Lehmann HI, Richter D, Prokesch H, et al. Atrioventricular node ablation in langendorff-perfused porcine hearts using carbon ion particle therapy methods and an in vivo feasibility investigation for catheter-free ablation of cardiac arrhythmias. *Circ-Arrhythm Electrophysiol*. 2015; 8(2): 429–438.

185. Perez-Castellano N, Villacastin J, Aragoncillo P, et al. Pathological effects of pulmonary vein beta-radiation in a swine model. *J Cardiovasc Electrophysiol*. 2006; 17(6): 662–669.

186. Lehmann HI, Deisher AJ, Takami M, et al. External arrhythmia ablation using photon beams ablation of the atrioventricular junction in an intact animal model. *Circ-Arrhythm Electrophysiol*. 2017; 10(4): e004304.

187. Sharma A, Wong D, Weidlich G, et al. Noninvasive stereotactic radiosurgery (CyberHeart) for creation of ablation lesions in the atrium. *Heart Rhythm*. 2010; 7(6): 802–810.

188. Hohmann S, Deisher AJ, Suzuki A, et al. Left ventricular function after noninvasive cardiac ablation using proton beam therapy in a porcine model. *Heart Rhythm*. 2019; 16(11): 1710–1719.

189. Krug D, Blanck O, Demming T, et al. Stereotactic body radiotherapy for ventricular tachycardia (cardiac radiosurgery) First-in-patient treatment in Germany. *Strahlenther Onkol*. 2020; 196(1): 23–30.

190. Jumeau R, Ozsahin M, Schwitter J, et al. Rescue procedure for an electrical storm using robotic non-invasive cardiac radio-ablation. *Radiother Oncol*. 2018; 128(2): 189–191.

191. Loo BW Jr, Soltys SG, Wang L, et al. Stereotactic ablative radiotherapy for the treatment of refractory cardiac ventricular arrhythmia. *Circ Arrhythm Electrophysiol*. 2015; 8(3): 748–750.

192. Cuculich PS, Schill MR, Kashani R, et al. Noninvasive cardiac radiation for ablation of ventricular tachycardia. *N Engl J Med.* 2017; 377(24): 2325–2336.

193. Neuwirth R, Cvek J, Knybel L, et al. Stereotactic radiosurgery for ablation of ventricular tachycardia. *Europace.* 2019; 21(7): 1088–1095.

194. Constantinescu A, Lehmann HI, Packer DL, Bert C, Durante M, Graeff C. Treatment planning studies in patient data with scanned carbon ion beams for catheter-free ablation of atrial fibrillation. *J Cardiovasc Electrophysiol.* 2016;27(3):335–344.

195. Goddu SM, Hilliard J, Knutson N, et al. Feasibility of noninvasive cardiac ablation utilizing intensity modulated proton therapy to treat ventricular tachycardia. *Int J Radia Oncol • Biol • Phys.* 2018; 102(3): S58.

196. ANSA. *Un fascio di protoni cura l'aritmia ventricolare, prima mondiale.* https://www.ansa.it/canale_saluteebenessere/notizie/medicina/2020/01/22/-protoni-curano-aritmia-ventricolare-prima-mondiale-_217fcc8e-9e0c-445b-8a20-575717520486.html

197. Rapp F, Simoniello P, Wiedemann J, et al. Biological cardiac tissue effects of high-energy heavy ions: investigation for myocardial ablation. *Sci Rep.* 2019;9:13.

198. Knutson NC, Samson PP, Hugo GD, et al. Radiation therapy workflow and dosimetric analysis from a phase 1/2 trial of noninvasive cardiac radioablation for ventricular tachycardia. *Int J Radiat Oncol Biol Phys.* 2019; 104(5): 1114–1123.

SUPPORTING INFORMATION

Additional supporting information may be found in the online version of the article at the publisher's website.

APPENDIX 1: CARDIAC MOTION

Cardiac motion has different implications in radiation oncology. Compared to respiratory motion discussed in 3.1, the frequency of cardiac motion (60–80 bpm) is much higher and the motion amplitude lower. Thus, cardiac motion-related dosimetric influence is less critical than respiration. But the heart is also influenced by respiratory motion, that is, the overall motion is a superimposition of cardiac and respiratory motion.[180] In daily clinical practice, the influence of cardiac motion is, thus, of minor importance in radiation oncology.

This conclusion changes when the heart is the primary target, as in ventricular tachycardia or atrial fibrillation treatments.[181] The method of choice for the treatment of severe disease progression is catheter ablation.[182] The rationale is the inactivation of arrhythmogenic areas in the heart or the isolation of the pulmonary veins in case of treatment of atrial fibrillation. Since catheter-based ablation is an invasive procedure and, thus, not always feasible due to comorbidities or not

always successful in reaching a persistent inactivation, other energy sources were investigated. Feasibility using radiation[183] has been shown several times, included in-vitro assessments,[184] in-vivo preclinical studies in swine for beta-radiation,[185] photons,[186] especially with clinical radiation therapy equipment,[187] protons,[188] as well as carbon therapy.[144] These data show that very high doses of 25–55 Gy in stereotactic radiosurgery setting are required to induce the functional endpoints such as interruption of cardiac impulse propagation or atrioventricular nodal block. The study using C-12 included 4D reconstruction (including cardiac motion) of the delivered dose.[146]

In parallel to these preclinical investigations, several centers started to treat individual patients who could not get cured with state-of-the-art treatment options with photon radiation therapy.[189,190]

The first case report of stereotactic ablative radiotherapy for the treatment of refractory cardiac ventricular arrhythmia by Loo et al. was published in 2015.[191] Cuculich et al. reported the first series of five patients treated by a standard C-arm linac with 25 Gy in a single session using a 4DCT-based ITV to account for cardiac and respiratory motion.[192] The clinical follow-up showed a 99.9% reduction of ventricular tachycardia (VT) episodes after a 4-week blanking period after treatment delivery. Similarly, Neuwirth et al.[193] reported on ten patients treated with a Cyberknife in 2014–2017. The cardiac motion was addressed by forming an ITV, while the respiratory motion was compensated with tracking by using the lead of the ICD as a fiducial marker. After receiving 25 Gy of treatment dose, the VT burden decreased by 87.5% compared to baseline for these patients.[193]

Treatment planning studies were used to assess the feasibility and potential benefit of proton and carbon therapy of arrhythmogenic lesions.[194,195] Data showed that the dose to normal tissues could be reduced compared to photon therapy and can be kept under the limits of radiation therapy. The study on carbon therapy involved 4D treatment planning and showed that interplay between the scanned beam and overlaid heart and respiratory motion can also be handled.

First proton therapy treatments were reported in early 2020. National Center of Oncological Hadrontherapy in Pavia, Italy, reports treatment of a 73-year-old patient who received treatment after IRB approval since drugs, invasive ablation, and cardiac denervation were not effective.[196]

Due to the complex setting and the relatively low number of reports, neither the underlying biology nor the most suitable motion-mitigation option is fully understood. Radiation-induced fibrosis and cardiomyocyte functional inactivation are discussed, but longer follow-up is needed.[190,197] Concerning motion management, ITV, motion tracking, and gating are being investigated.[198] Thus, several avenues for future

research exist, in particular for particle-beam therapy. However, this report will not discuss cardiac motion further because of the limited data available.

APPENDIX 2: SURVEYS ON MOTION MANAGEMENT FOR PARTICLE THERAPY

Three surveys on topics related to motion management for particle therapy were conducted via private communication in 2014, 2016, and 2018, with 10, 14, and 13 institutions responding in the respective years (previously unpublished, conducted by Dr. Antje Knopf in 2014, and Dr. Stella Flampouri in 2016 and 2018). While the emphasis of the surveys differed—the 2014 survey focused on delivery techniques, the 2016 survey focused on stereotactic body radiation therapy (SBRT), and the 2018 survey focused on plan robustness—a consensus in clinical practice and paradigms emerged by the compilation of the surveys (Supporting information Table S1).

The survey results suggested that the respondents' confidence in using PBS with moving targets increased with recent technological advancements. Despite the increased delivery time, rescanning has become a popular option for PBS delivery owing to its simplicity. In the SBRT setting, active motion management is critical because it effectively reduces target volume compared to geometric expansions and reduces the interplay effect by effectively reducing the motion range. 4DCT and repeated CT are essential in monitoring intrafractional and interfraction motion, respectively.